Geoscience Frontiers 4 (2013) 423–438

Contents lists available at SciVerse ScienceDirect

China University of Geosciences (Beijing)

Geoscience Frontiers

journal homepage: www.elsevier.com/locate/gsf

Research paper

Petrogenesis of the late Cretaceous Turnagöl intrusion in the eastern Pontides: Implications for magma genesis in the arc setting

Abdullah Kaygusuz [a,*], Ferkan Sipahi [a], Nurdane İlbeyli [b], Mehmet Arslan [c], Bin Chen [d], Emre Aydınçakır [a]

[a] Department of Geological Engineering, Gümüşhane University, TR-29000 Gümüşhane, Turkey
[b] Department of Geological Engineering, Akdeniz University, TR-070058 Antalya, Turkey
[c] Department of Geological Engineering, Karadeniz Technical University, TR-61080 Trabzon, Turkey
[d] Department of Geological Engineering, Peking University, Beijing 100871, China

A R T I C L E I N F O

Article history:
Received 3 July 2012
Received in revised form
27 September 2012
Accepted 28 September 2012
Available online 29 October 2012

Keywords:
Turnagöl intrusion
Late Cretaceous
Sr-Nd-Pb-O isotope
U-Pb zircon dating
Eastern Pontides
Turkey

A B S T R A C T

A series of Cretaceous plutons is present in the eastern Pontides of northeastern Turkey. The Turnagöl intrusion is the least studied and, thus, the least understood plutons in the orogen. This intrusion consists of hornblende-biotite granodiorites emplaced at 78 Ma based on LA-ICP-MS U-Pb zircon dating. It is of sub-alkaline affinity, belongs to the medium- to high-K calc-alkaline series, and displays features typical of I-type granites. The rocks of the intrusion are enriched in large-ion lithophile elements and light rare earth-elements with negative Eu anomalies (Eu/Eu* $= 0.69$–0.82), but are deficient in high-field-strength elements. They have a small range of $(^{87}Sr/^{86}Sr)_i$ (0.7060–0.7063), ε_{Nd_i}(-2.6 to -3.1), and $\delta^{18}O$ ($+8.1$ to $+9.1$) values. Their Pb isotopic ratios are $^{206}Pb/^{204}Pb = 18.63$–$18.65$, $^{207}Pb/^{204}Pb = 15.62$–$15.63$, and $^{208}Pb/^{204}Pb = 38.53$–$38.55$. The fractionation of plagioclase, hornblende, and Fe-Ti oxides had key functions in the evolution of the Turnagöl intrusion. The crystallization temperatures of the melts ranged from 758 to 885 °C as determined by zircon and apatite saturation thermometry. All these characteristics, combined with the low values of K_2O/Na_2O and $(Na_2O + K_2O)/(FeO^t + MgO + TiO_2)$, as well as the high values of $(CaO + FeO^t + MgO + TiO_2)$, suggest an origin by dehydration melting from a metabasaltic lower crustal source.

1. Introduction

Turkey is located on an east-west trending segment of the Alpine-Himalayan orogenic belt. This belt embraces various arc-, collision-, and post-collision geologic settings. In this belt, Turkey, as the zone of interaction between the Eurasia and Gondwanaland plates, lies in an important geodynamic position. The Pontide unit (Ketin, 1966) of Turkey includes various intrusive and eruptive rocks that constitute the widespread eastern Pontide Terrane, many of which are related to the convergence of these two plates (Fig. 1A).

* Corresponding author. Tel.: +90 456 2337425; fax: +90 456 2337427.
E-mail address: abdullah.kaygusuz@gmail.com (A. Kaygusuz).

Peer-review under responsibility of China University of Geosciences (Beijing)

Production and hosting by Elsevier

The crystallization ages of these intrusive rocks range from the Permo-Carboniferous (Çoğulu, 1975; Topuz et al., 2004, 2010; Dokuz, 2011; Kaygusuz et al., 2012) through the Cretaceous–Paleocene (Yılmaz et al., 2000; Boztuğ et al., 2006; İlbeyli, 2008; Kaygusuz et al., 2008, 2009, 2010; Kaygusuz and Aydınçakır, 2009; Karslı et al., 2010; Kaygusuz and Şen, 2011) to the Eocene periods (Boztuğ et al., 2004; Topuz et al., 2005; Yılmaz-Şahin, 2005; Arslan and Aslan, 2006; Karslı et al., 2007; Eyuboğlu et al., 2011b). The rocks were formed in different geodynamic environments, and the emplacements of these plutons occurred in a wide range of tectonic settings: from arc-collisional, through syn-collisional, to post-collisional (e.g., Yılmaz and Boztuğ, 1996; Okay and Şahintürk, 1997; Yılmaz et al., 1997; Yeğingil et al., 2002; Boztuğ et al., 2003).

Investigations on the intrusive rocks of the eastern Pontides are extensive (e.g., Delaloye et al., 1972; Yılmaz, 1972; Taner, 1977; Gedikoğlu, 1978; Moore et al., 1980; Jica, 1986; Yılmaz and Boztuğ, 1996; Okay and Şahintürk, 1997; Karslı et al., 2004; Boztuğ et al., 2004, 2006; Yılmaz-Şahin et al., 2004; Topuz et al., 2005; Yılmaz-Şahin, 2005; Dokuz et al., 2006; Kaygusuz et al., 2008, 2009, 2010, 2011, 2012). However, studies on the Turnagöl intrusion are limited

1674-9871/$ – see front matter © 2012, China University of Geosciences (Beijing) and Peking University. Production and hosting by Elsevier B.V. All rights reserved.
http://dx.doi.org/10.1016/j.gsf.2012.09.003

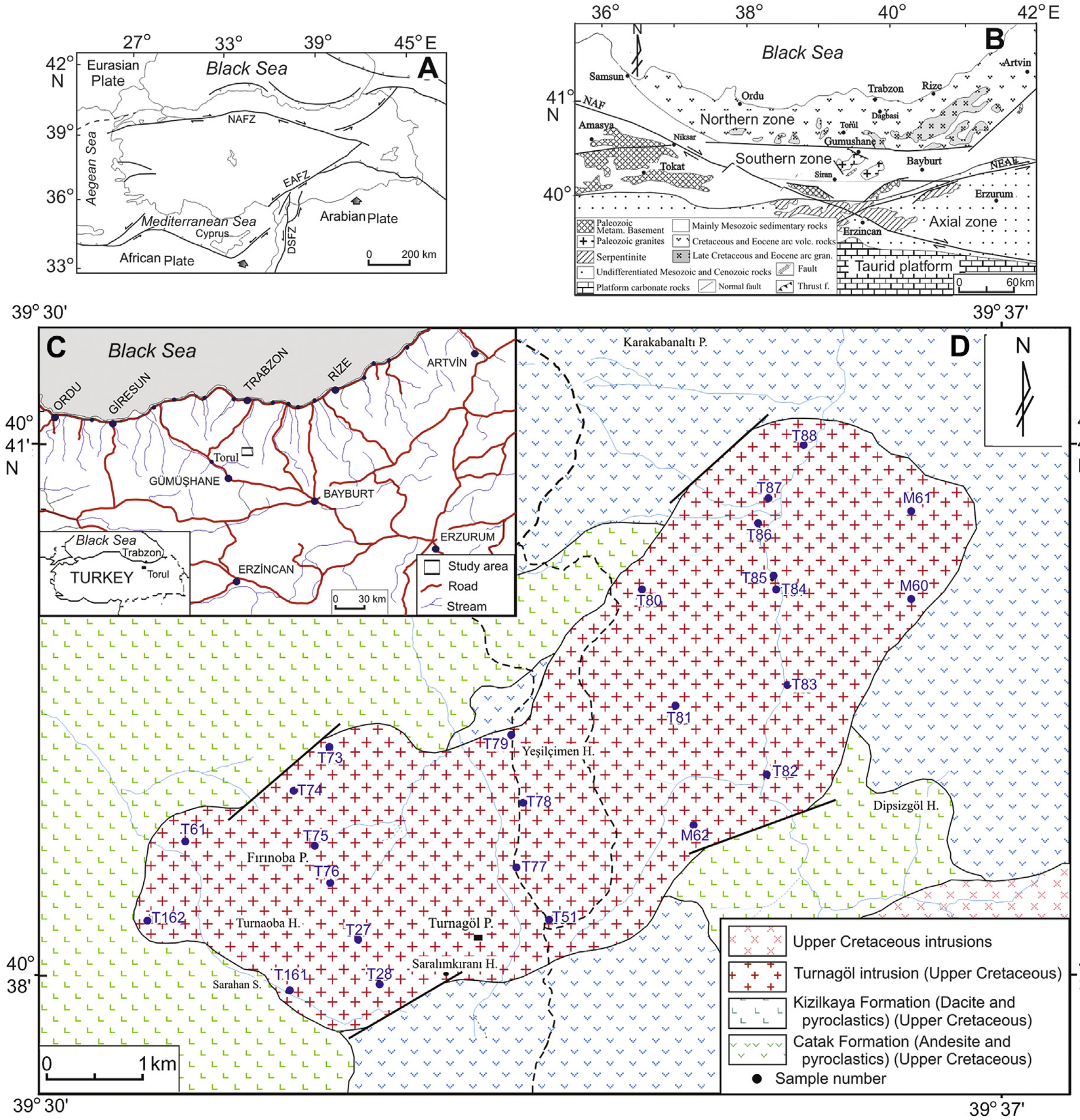

Figure 1. (A) Tectonic map of Turkey and surroundings (modified after Şengör et al., 2003); (B) Major structures of the eastern Pontides (modified from Eyuboğlu et al., 2007); (C) Location map of the study area and (D) Geological map of the study area. NAFZ: North-Anatolian fault zone; EAFZ: East-Anatolian fault zone; DSFZ: Dead Sea fault zone.

and primarily related to mine as well as general geological research (Yalçınalp, 1992; Güven, 1993). The present study examines the Turnagöl intrusion, which is geochemically and isotopically the least-studied series of plutons in the eastern Pontides. Before this study, the age of the Turnagöl intrusion has been uncertain, and no geochronological age of this intrusion is currently available. In this article, new petrographic, geochemical, Sr-Nd-Pb-O isotopic, and LA-ICP-MS U-Pb zircon data from the Turnagöl intrusion in the eastern Pontide magmatic arc are reported. These geochemical and isotopic data reveal the magma sources and magma production processes of the I-type, calc-alkaline granitoids from the eastern Pontides.

2. Geological background

The eastern Pontides orogenic belt is located within the Alpine metallogenic belt, and geographically corresponds to the eastern Black Sea region of Turkey. It is commonly subdivided into northern and southern zones (Fig. 1B) based on structural and lithological features (Özsayar et al., 1981; Okay and Şahintürk, 1997). These zones have different lithological characteristics and are separated by E–W, NE–SW, and NW–SE oriented fault zones that define the block-faulted tectonic style of the eastern Pontides (Bektaş and Çapkınoğlu, 1997). The late Cretaceous and middle Eocene volcanic and volcaniclastic rocks dominate the northern zone, whereas pre-late Cretaceous rocks dominate the southern zone (Arslan et al., 1997, 2000; Şen et al., 1998; Şen, 2007; Temizel et al., 2012). The basement of the eastern Pontides consists of early Carboniferous metamorphic rocks (Topuz et al., 2004, 2007), and is crosscut by granitoids of late Carboniferous age (Yılmaz, 1972; Çoğulu, 1975; Okay and Şahintürk, 1997; Topuz et al., 2010; Dokuz, 2011; Kaygusuz et al., 2012). The early Jurassic volcanic rocks of the eastern Pontides unconformably lie on a Paleozoic heterogeneous crystalline basement, and are crosscut by younger granitoids of Jurassic to Paleocene age (Okay and Şahintürk, 1997; Dokuz et al., 2006; Kaygusuz et al., 2008, 2009, 2010; Karslı et al., 2010). Volcanic and volcano-sedimentary rocks of early and middle

Jurassic ages are tholeiitic in character (Arslan et al., 1997; Şen, 2007). They are conformably overlain by middle–late Jurassic–Cretaceous neritic and pelagic carbonates. The late Cretaceous series that unconformably overlies these carbonate rocks consists of sedimentary rocks in the southern part, and of volcanic rocks in the northern part (Bektaş et al., 1987; Robinson et al., 1995; Yılmaz and Korkmaz, 1999). The Cretaceous volcanic rocks mainly belong to the tholeiitic and calc-alkaline series, and host several volcanogenic massive sulphide deposits (Akçay et al., 1998). The Eocene volcanic and volcaniclastic rocks unconformably overlie the late Cretaceous volcanic and/or sedimentary rocks (Güven, 1993; Yılmaz and Korkmaz, 1999), and are intruded by calc-alkaline granitoids of similar age (Arslan and Aslan, 2006; Karslı et al., 2007; Eyuboğlu et al., 2011b). Post-Cretaceous magmatic rocks include the Paleocene plagioleucitites (Altherr et al., 2008; Eyuboğlu, 2010), early Eocene "adakitic" granitoids (Topuz et al., 2005; Eyuboğlu et al., 2011a, b, c, d), as well as middle–late Eocene calc-alkaline to tholeiitic, basaltic to andesitic volcanic rocks, and crosscutting granitoids exposed throughout the eastern Pontides (e.g., Tokel, 1977; Arslan et al., 1997; Karslı et al., 2007; Boztuğ and Harlavan, 2008; Temizel and Arslan, 2009; Temizel et al., 2012). The post-Eocene uplift and erosion brought clastic input into the locally developed basins (Korkmaz et al., 1995). From the end of the middle Eocene, the region remained largely above sea level, with minor volcanism and terrigenous sedimentation that continue to the present-day (Okay and Şahintürk, 1997). The Miocene and post-Miocene volcanic history of the eastern Pontides is characterized by calc-alkaline to mildly alkaline volcanism (Aydın, 2004; Yücel et al., 2011; Temizel et al., 2012) and the late Miocene adakitic magmatism (Eyuboğlu et al., 2012).

The study area is located in the northern zone of the eastern Pontides (Fig. 1C). The basement rocks consist of Paleozoic granites (Kaygusuz et al., 2012). The granites are unconformably overlain by early Jurassic volcanics that consist of basalts, andesites, and their pyroclastic equivalents. These rocks are conformably overlain by middle–late Jurassic–Cretaceous carbonates. These carbonates are conformably overlain by late Cretaceous basic and acidic volcanic rocks consisting of andesites, dacites, and their pyroclastic equivalents interbedded with sedimentary layers. All these lithologies are cut by late Cretaceous granitoids. According to field observations, the Turnagöl intrusion cuts late Cretaceous formations, and is cut by aplitic, dacitic, as well as andesitic dykes. The intrusion was dated as 78.07 ± 0.73 Ma using U-Pb zircon dating on granodiorite in this study.

3. Analytical methods

3.1. Whole-rock major and trace element analyses

Twenty-five samples were collected from the Turnagöl intrusion (for sample location see Fig. 1D). On the basis of the petrographical studies, 10 of the freshest and most representative rock samples from the intrusion were selected for whole-rock major-, trace- and rare earth-element (REE) analyses. Rock samples were crushed in steel crushers and grinded in an agate mill to a grain size of <200 mesh. Major, trace and REE analyses were carried out at ACME Analytical Laboratories Ltd., Vancouver, Canada. Major and trace element compositions were determined by ICP-MS after 0.2 g samples of rock powder were fused with 1.5 g $LiBO_2$ and then dissolved in 100 mL 5% HNO_3. REE contents were analyzed by ICP-MS after 0.25 g samples of rock powder were dissolved by four acid digestion steps. Loss on ignition (LOI) is by weight difference after ignition at 1000 °C. Total iron concentration is expressed as Fe_2O_3. Detection limits range from 0.002 wt.% to 0.04 wt.% for major oxides, from 0.1 to 8 ppm for trace elements, and from 0.01 to 0.3 ppm for REE.

3.2. Zircon U-Pb dating

Zircon grains were extracted by heavy-liquid and magnetic separation methods, and further purified by hand-picking under a binocular microscope. Selected grains were mounted in an epoxy resin and polished until half way through. Cathodoluminescence (CL) images were acquired to check the internal structures of individual zircon grains and to ensure a better selection of analytical positions.

U-Pb zircon dating was carried out by using LA-ICP-MS at the Geologic Lab Center, China University of Geosciences (Beijing). A quadrupole ICP-MS (Agilent 7500a) was connected with a UP-193 Solid-state laser (193 nm, New Wave Research Inc.) with an automatic positioning system. Laser spot size was set to ~36 μm, and the energy density at 8.5 J/cm^2 and repetition rate at 10 Hz. The procedure of laser sampling was 5 s pre-ablation, 20 s sample-chamber flushing and 40 s sampling ablation. The ablated material was carried into the ICP-MS by a high-purity He gas stream with flux of 0.8 L/min. The whole laser path was fluxed with N_2 (15 L/min) and Ar (1.15 L/min) in order to increase energy stability. U-Pb isotope fractionation effects were corrected using zircon 91500 (Wiedenbeck et al., 1995) as external standard. Zircon standard TEMORA (417 Ma, Black et al., 2003) was also used as a secondary standard to monitor the deviation of age measurement/calculation. Ten analyses of TEMORA yielded apparent $^{206}Pb/^{238}U$ ages of 417–418 Ma. Isotopic ratios and element concentrations of zircons were calculated using the GLITTER software (ver. 4.4, Macquarie University). Concordia ages and diagrams were obtained using Isoplot/Ex 3.0 (Ludwig, 2003). Common lead was corrected following the method of Andersen (2002).

3.3. Sr-Nd-Pb isotope analyses

Sr, Nd and Pb isotope compositions were measured on a Finnigan MAT 262 multicollector mass spectrometer at the Institute of Geosciences, Tübingen (Germany). For Sr-Nd isotope analyses, approximately 50 mg of whole-rock powder was decomposed in 52% HF for 4 days at 140 °C on a hot plate. Digested samples were dried and redissolved in 6 N HCl, dried again and redissolved in 2.5 N HCl. Sr and Nd were separated by conventional ion exchange techniques and their isotopic compositions were measured on single W and double Re filament configurations, respectively. The isotopic ratios were corrected for isotopic mass fractionation by normalizing to $^{86}Sr/^{88}Sr = 0.1194$ and $^{146}Nd/^{144}Nd = 0.7219$. The reproducibility of $^{87}Sr/^{86}Sr$ and $^{143}Nd/^{144}Nd$ during the period of measurement was checked by analyses of NBS 987 Sr and La Jolla Nd standards yielding average values of 0.710235 ± 0.000015 (2SD, $n = 3$) and 0.511840 ± 0.000008 (2SD, $n = 5$), respectively. Total procedural blanks were 20–50 pg for Sr and 40–66 pg for Nd. Separation and purification of Pb was carried out on Teflon columns with a 100 μL (separation) and 40 μL bed (cleaning) of Bio-Rad AG1-X8 (100–200 mesh) anion exchange resin using a HBr-HCl ion exchange procedure. Pb was loaded with Si-gel and phosphoric acid onto a Re filament and was analyzed at ~1300 °C in single-filament mode. A factor of 1‰ per atomic mass unit for instrumental mass fractionation was applied to the Pb analyses, using NBS SRM 981 as reference material. Total procedural blanks for Pb during the measurement period were between 20 and 40 pg. Sample reproducibility is estimated at ±0.02, ±0.015 and ±0.03 (2σ) for $^{206}Pb/^{204}Pb$, $^{207}Pb/^{204}Pb$ and $^{208}Pb/^{204}Pb$ ratios, respectively.

3.4. $\delta^{18}O$ isotope analyses

For stable isotopes, oxygen was extracted using the BrF_5 method of Clayton and Mayeda (1963), and the $\delta^{18}O$ values were measured using a dual-inlet Finnigan MAT 252 isotopic ratio mass spectrometer at Queen's University, Canada. The O isotope compositions are reported in the δ notation in units of per mil relative to the standard V-SMOW. The $\delta^{18}O$ and δD values were reproducible to ±0.2 and ±3 per mil, respectively. The oxygen isotope fractionation factors used throughout this paper are those proposed by Wenner and Taylor (1971) for water-chlorite, O'Neil and Taylor (1969) for water-muscovite, as well as Fayek and Kyser (2000) for water-uraninite. In previous studies, the water-illite fractionation factor was used instead of water-muscovite. The δD values of the fluids were 38 per mil higher at 250 °C using the muscovite-water fractionation factors relative to those using illite-water. Therefore, we preferred the muscovite-water fractionation factor of Vennemann and O'Neil (1996).

4. Field and microscopic observation

The Turnagöl intrusion is located about 35 km southwest of Trabzon and exhibits an NE–SW elongated shape (Fig. 1C and D). The intrusion covers an area of approximately 25 km^2. Similar plutons are seen to the east and southern west of the Turnagöl intrusion, around the Camiboğazı and Torul regions. The Turnagöl intrusion cuts the late Cretaceous andesitic rocks (Çatak Formation) in the northeast and the dacitic rocks in the southwest (Kızılkaya Formation). The contacts between the Turnagöl intrusion and the country rocks are predominantly sharp and discordant. The contact facies are finer-grained, and the shape of the pluton is elliptic. The textures are massive, porphyritic, and granophyric; the granitoids contain country rock xenoliths at the endocontact. In the eastern part of the intrusion, a number of mafic microgranular enclaves with ellipsoidal shapes (up to 10 cm in diameter) occur. Their contacts with the host granodiorites vary from sharp to gradational. The granodiorites are gray to light gray and have a fine- to medium-grained texture, which is feldspar porphyritic near the contact to the country rocks. These are generally undeformed, slightly altered, and minimally weathered. Most rocks are brick red to pink, and a few are greenish chloritized zones.

The rock samples are generally holocrystalline, fine- to medium-grained, porphyric, poikilitic, myrmekitic, and rarely micrographic in texture. Toward the contact with the volcanic country rocks, the granitoids possess fine-grained textures; toward the center of the intrusion, the medium-grained textures predominate. Porphyric textures are generally seen close to the contact of the volcanic country rocks. The intrusion contains mainly plagioclase, quartz, K-feldspar, biotite, and hornblende. The accessory phases include titanite, allanite, apatite, zircon, epidote, and some opaque minerals. The secondary minerals comprise chlorite, calcite, sericite, and clay minerals.

The plagioclase mostly forms subhedral to anhedral, normally and reversely zoned prismatic, lath-shaped crystals. The grain sizes vary from 0.2 mm for inclusions to 3 mm for large crystals. Plagioclase shows oscillatory zoning, albite twinning, and prismatic-cellular growth. A myrmekitic texture is observed at the grain boundaries between orthoclase and plagioclase. Some plagioclase crystals have poikilitic textures, in which large plagioclase crystals (up to 3 mm) may contain small crystals of plagioclase, hornblende, and biotite. Some large plagioclase crystals are altered to sericite and clay minerals. The quartz is anhedral in shape and fills interstices between other minerals. It generally shows undulose extinction and its grain size becomes increasingly smaller in the contact zones between the country rocks. The K-feldspar forms anhedral, rarely subhedral, crystals of perthitic orthoclase. The alteration to clay minerals is more common in the large K-feldspar crystals than in plagioclase. The biotite is abundant in all samples. It is euhedral and subhedral, reddish-brown, and forms prismatic crystals as well as lamellas. In some samples, biotite is altered into chlorite, epidote, or an opaque mineral along its cleavage planes. The hornblende occurs as small euhedral to subhedral, tablet-like prismatic crystals, with some minerals that are altered into chlorite, calcite, and actinolite. Large hornblende crystals (up to 2.5 mm) may contain small plagioclase and biotite inclusions. The titanite forms euhedral and subhedral crystals in all rocks. The allanite occurs as reddish, euhedral crystals in all rocks. The needle-like crystals of apatite are mainly found in plagioclase. Euhedral zircon is an accessory phase in all rocks and forms short prismatic crystals.

5. Major and trace element geochemistry

The results of the major, trace, and rare earth-element (REE) analyses of representative samples from the Turnagöl intrusion are shown in Tables 1 and 2. In the classification diagram of Middlemost (1994), all samples are found in the granodiorite field (Fig. 2). The granodiorites span a narrow compositional range with $w(SiO_2)$ between 67% and 70%, as well as a low $Mg^{\#}$ (22–28) (Table 1; Fig. 2). Their K_2O/Na_2O ratios vary between 0.59 and 0.87. The aluminium saturation index (ASI = A/CNK) (molar Al_2O_3/($CaO + Na_2O + K_2O$)) values of samples from the Turnagöl intrusion are between 0.97 and 1.11, indicating that the granodiorites are peraluminous to slightly metaluminous (Table 1; Fig. 3A). Some altered samples from the Turnagöl intrusion portray elevated ASI values. They show sub-alkaline affinity and belong to the medium- to high-K calc-alkaline series (Fig. 3B). Harker plots of the selected major and trace elements (Fig. 4A–R) show the systematic variations in the element concentrations. The rocks define trends without a compositional gap. The CaO, MgO, Al_2O_3, $Fe_2O_3^t$, TiO_2, and P_2O_5 abundances decrease with increasing SiO_2, whereas K_2O and Na_2O increase (Fig. 4A–H). Ba, Rb, Th, Pb, and Nb show a positive linear trend, whereas Sr, Ni, and Eu define a negative correlation with increasing SiO_2 content (Fig. 4J–O, and 4Q–R). Zr and Y remain nearly constant (Fig. 4I and P).

6. REE geochemistry

The general trends of the primitive mantle-normalized (Sun and McDonough, 1989) element concentration diagrams are shown in Fig. 5A. All rocks show the enrichment of large-ion lithophile elements (LILEs) and the depletion of high-field-strength elements (HFSEs). The depletion in HFSEs is best expressed by the negative Nb, Ta, P, and Ti anomalies. Positive Pb anomalies are seen in the samples (Fig. 5A).

The chondrite-normalized (Taylor and McLennan, 1985) REE patterns of the Turnagöl samples (Fig. 5B) are generally characterized by concave-upward shapes (La_{cn}/Yb_{cn} = 7.1–9.3) and pronounced negative Eu anomalies (Eu_{cn}/Eu^*) of 0.69–0.82 (Table 2).

7. Temperatures

The apatite and zircon saturation temperatures (Watson and Harrison, 1983; Harrison and Watson, 1984; Hanchar and Watson, 2003; Miller et al., 2003) calculated from the bulk-rock chemical analyses of rock samples correspond to the maximum or minimum temperature limits for the intruding magma, depending on whether the melt was saturated or undersaturated with these components. The Zr abundances in granodiorite samples from the Turnagöl intrusion (122–135 ppm; Table 1) result in zircon saturation temperatures of 758–773 °C. Subhedral zircon grains do not occur in the cores of the large plagioclase and hornblende grains, but are abundant in quartz, orthoclase, biotite, and the outer parts

Table 1
Whole-rock major (wt.%) and trace (ppm) element analyses of representative samples and zircon and apatite crystallization temperatures from the Turnagöl intrusions.

Rock types	Granodiorites									
	T84	T86	T162	T88	T28	T76	T82	T73	T51	T78
SiO_2	67.27	67.50	67.56	68.05	68.62	68.64	69.09	69.17	69.22	70.16
TiO_2	0.38	0.38	0.35	0.33	0.35	0.33	0.34	0.32	0.33	0.31
Al_2O_3	15.54	15.01	15.41	15.25	14.21	14.92	14.91	14.79	14.69	14.67
$Fe_2O_3^t$	4.15	4.01	3.65	3.48	3.61	3.43	3.37	3.31	3.37	3.25
MnO	0.12	0.10	0.12	0.07	0.07	0.08	0.06	0.07	0.10	0.07
MgO	1.65	1.56	1.25	1.11	1.18	1.36	0.95	1.17	1.19	1.01
CaO	3.71	3.64	3.03	3.75	2.33	2.62	3.73	2.73	2.29	2.13
Na_2O	3.34	3.53	3.42	3.53	4.19	3.50	3.35	3.54	3.67	3.78
K_2O	2.09	2.10	2.59	2.74	3.11	2.97	2.80	2.98	3.14	3.30
P_2O_5	0.10	0.09	0.10	0.09	0.09	0.08	0.09	0.09	0.08	0.07
LOI	1.60	1.90	2.30	1.40	2.00	1.90	1.10	1.70	1.70	0.80
Total	99.95	99.82	99.78	99.80	99.76	99.83	99.79	99.87	99.78	99.55
Ni	2.1	1.6	1.1	1.2	1.5	1	1.4	1.0	1.1	0.9
V	95	66	55	55	50	56	53	55	64	47
Cu	6.8	2.2	1.8	3.7	3	3.2	3.1	1.9	4.7	4.5
Pb	8.4	6.4	5.3	7.5	23.2	9.6	13.4	10.2	6.3	20.1
Zn	47	34	45	25	35	34	25	29	28	22
W	1.2	1.5	1.3	1.2	1	1.2	0.9	0.6	1.1	2.4
Rb	50.8	51.5	57	75.1	70.6	71	75.2	75.5	80	88.1
Ba	930	1011	1237	1085	1086	1082	1126	1142	1198	1151
Sr	259.3	237.1	272.6	256.7	274.2	226.3	247.3	238.3	232.1	236.4
Ta	0.5	0.4	0.5	0.5	0.5	0.5	0.4	0.5	0.5	0.6
Nb	5.1	6.1	6.2	5.8	7.4	6.5	5.5	6.8	6.8	7.8
Hf	4.1	3.4	3.3	3.9	3.6	4	3.3	3.6	3.8	4.3
Zr	127.7	128.1	122.1	134.8	125.7	127.2	128.8	125.5	128.4	131.7
Y	19.6	17.6	20.3	17.2	24	20.3	15.1	20.6	20.9	20.4
Th	10	10.1	9.8	12	13.3	11.3	11.1	14.1	13.2	15.1
U	3.2	2.4	2.8	2.6	3.6	2.5	2.3	3.1	3.2	3.4
Ga	14.1	13.9	13.4	14.1	11.7	12.3	13	13.1	12.5	12.9
K_2O/Na_2O	0.63	0.59	0.76	0.78	0.74	0.85	0.84	0.84	0.86	0.87
K/Rb	341.5	338.5	377.2	302.9	365.7	347.3	309.1	327.7	325.8	310.9
K/Ti	7.65	7.69	10.30	11.55	12.36	12.52	11.46	12.96	13.24	14.81
Rb/Sr	0.20	0.22	0.21	0.29	0.26	0.31	0.30	0.32	0.34	0.37
Sr/Y	13.23	13.47	13.43	14.92	11.43	11.15	16.38	11.57	11.11	11.59
ASI	1.07	1.02	1.11	0.98	0.98	1.09	0.97	1.06	1.08	1.07
$Mg^{\#}$	28.45	28.01	25.51	24.18	24.63	28.39	21.99	26.12	26.10	23.71
Zircon (°C)	766	762	767	762	758	770	759	766	771	773
Apatite (°C)	876	867	879	873	879	868	884	885	874	871

$Fe_2O_3^t$ is total iron as Fe_2O_3, LOI is loss on ignition, $Mg^{\#}$ (Mg-number) = $100 \times MgO/(MgO + Fe_2O_3^t)$.
ASI = molar $Al_2O_3/(CaO + Na_2O + K_2O)$.
Watson and Harrison (1983) formulation used to calculate temperatures from zircon, and Harrison and Watson (1984) formulation used to calculate temperatures from apatite.

Table 2
Rare earth-element analyses (ppm) from the Turnagöl intrusions.

Rock types	Granodiorites									
	T84	T86	T162	T88	T28	T76	T82	T73	T51	T78
La	23.80	22.60	25.40	22.30	26.00	26.80	25.10	27.40	25.70	28.50
Ce	45.60	44.80	43.10	43.80	47.10	47.90	45.50	50.40	47.50	49.40
Pr	5.07	4.48	4.57	4.40	4.96	5.03	4.45	5.14	4.85	5.09
Nd	16.70	16.10	17.20	16.00	17.50	18.90	15.10	19.70	17.30	16.90
Sm	3.12	2.89	3.07	2.95	3.44	3.11	3.16	3.09	3.12	3.18
Eu	0.76	0.77	0.77	0.76	0.75	0.76	0.73	0.71	0.72	0.73
Gd	2.52	2.79	2.93	2.83	3.14	3.03	2.92	2.97	3.02	3.05
Tb	0.54	0.48	0.51	0.48	0.50	0.50	0.51	0.50	0.52	0.52
Dy	3.01	2.73	2.97	2.81	2.76	3.00	2.83	2.93	3.03	3.02
Ho	0.70	0.60	0.63	0.62	0.66	0.64	0.68	0.66	0.68	0.64
Er	2.03	1.88	1.90	1.80	2.06	2.01	1.93	1.96	2.06	1.99
Tm	0.32	0.27	0.30	0.28	0.32	0.31	0.32	0.34	0.32	0.33
Yb	2.28	2.01	2.05	1.98	2.15	2.11	2.13	2.14	2.23	2.08
Lu	0.37	0.33	0.32	0.31	0.33	0.33	0.32	0.36	0.35	0.35
$(La/Lu)_{cn}$	6.66	7.09	8.22	7.45	8.16	8.41	8.12	7.88	7.60	8.43
$(La/Sm)_{cn}$	4.80	4.92	5.21	4.76	4.76	5.42	5.00	5.58	5.18	5.64
$(Gd/Lu)_{cn}$	0.85	1.05	1.14	1.13	1.18	1.14	1.13	1.02	1.07	1.08
$(La/Yb)_{cn}$	7.05	7.60	8.37	7.61	8.17	8.58	7.96	8.65	7.79	9.26
$(Tb/Yb)_{cn}$	1.01	1.02	1.06	1.04	0.99	1.01	1.02	1.00	1.00	1.07
Eu/Eu^*	0.80	0.82	0.77	0.79	0.69	0.75	0.72	0.71	0.71	0.71

$Eu^* = (Sm + Gd)_{cn}/2$.

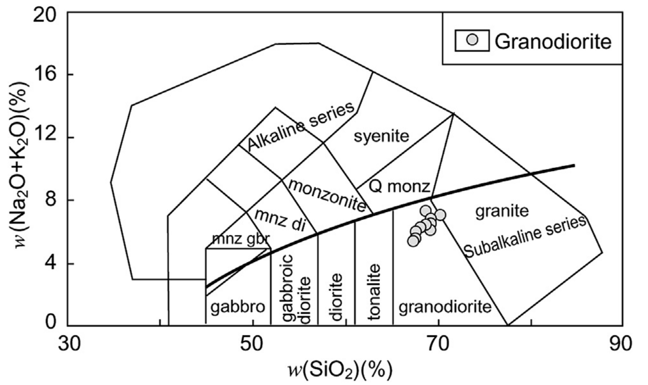

Figure 2. Chemical nomenclature diagram (Middlemost, 1994) for samples from the Turnagöl intrusion. mnz gbr: monzogabbro; mnz di: monzodiorite; Q monz: quartz monzonite.

of plagioclase grains. Thus, the crystallization of zircon started relatively late at temperatures lower than that of the intruding magma. This conclusion is supported by the fact that the Zr abundances are not systematically related to the SiO_2 concentration (Fig. 4I). Therefore, the calculated zircon saturation temperatures should be considerably lower than the temperature of the intruding magma. On the other hand, apatite crystallization seems to have started earlier because the apatite grains occur in early crystallized plagioclase and hornblende (as well as in other phases), and the bulk-rock P_2O_5 content decreases with increasing SiO_2 (Fig. 4H). Therefore, the temperatures of the intruding magmas were probably not much higher than the calculated apatite saturation temperatures of 867–885 °C.

8. U-Pb zircon dating

The LA-ICP-MS U-Pb zircon dating results are presented in Table 3 and shown as Concordia diagrams in Fig. 6. A granodiorite, sample T86, from the Turnagöl intrusion contains abundant zircon grains. Zircons are colorless, short to long prismatic, and perfectly euhedral (Fig. 6A). The zircon grains are mostly fine-grained (70–150 μm) and have aspect ratios of about 1–3. They exhibit pyramidal terminations and oscillatory zoning (Fig. 6A). All these features indicate that zircons are of magmatic origin (Pupin, 1980). About 20 points were analyzed from different crystals. For U-Pb isotope analyses, only the uncorroded inner parts of the grains were investigated. Most analyses give concordant age data. Twenty spots from sample T86 yield $^{206}Pb/^{238}U$ ages ranging from 75 to 81 Ma with a weighted mean age of 78.07 ± 0.73 Ma (MSWD = 0.96) (Table 3; Fig. 6B and C). Thus, a late Cretaceous age is established for the intrusion by U-Pb zircon dating, and this age is interpreted as the magmatic emplacement age. These results are in agreement with stratigraphical and geological observations, which indicate that the I-type Turnagöl intrusion intruded into the late Cretaceous volcanic rocks in the region (Fig. 1D).

9. Sr, Nd and Pb isotopes

Sr, Nd and Pb isotopic data for the Turnagöl intrusion are listed in Tables 4 and 5, and plotted in Fig. 7. The initial Sr, Nd and Pb isotope ratios were calculated using the Rb, Sr, Sm, Nd, U, Th and Pb concentration data obtained from ICP-MS analyses, by assuming a granodiorite age of 78 Ma (see below). Samples from the Turnagöl intrusion show a narrow range of initial $^{87}Sr/^{86}Sr$ ratios (0.7060–0.7063) and ε_{Nd_i} values (−2.6 to −3.1). The corresponding Nd model ages (T_{DM}) of the granites range from 1.11 to 1.16 Ga. As illustrated in Fig. 7A, the samples plot within the right quadrants of a conventional Sr-Nd isotope diagram.

In the SiO_2 vs. $(^{87}Sr/^{86}Sr)_i$ and $(^{143}Nd/^{144}Nd)_i$ diagrams (Fig. 7B and C, respectively), the samples define nearly horizontal trends that indicate fractional crystallization (FC). However, a slightly positive correlation is shown in the $(^{87}Sr/^{86}Sr)_i$ vs. MgO plot (Fig. 7D).

In Fig. 7A, the Turnagöl intrusion is compared with other Cretaceous plutons from the eastern Pontides. The studied samples have ε_{Nd_i} and $(^{87}Sr/^{86}Sr)_i$ ratios similar to those from Torul and Sarıosman plutons, but have lower $(^{87}Sr/^{86}Sr)_i$ ratios than those from the Dağbaşı pluton. The Dağbaşı, Torul, Sarıosman, Köprübaşı, and Harşit samples show a negative correlation between ε_{Nd_i} and $(^{87}Sr/^{86}Sr)_i$, whereas the Turnagöl samples show no obvious correlation between these two parameters.

The samples from the Turnagöl intrusion have similar isotopic compositions: $(^{206}Pb/^{204}Pb)_i$ = 18.63–18.65, $(^{207}Pb/^{204}Pb)_i$ = 15.62–15.63, and $(^{208}Pb/^{204}Pb)_i$ = 38.53–38.55 (Table 5; Fig. 7E and F). In the $(^{207}Pb/^{204}Pb)_i$ vs. $(^{206}Pb/^{204}Pb)_i$ diagram (Fig. 7E), the samples plot to the left of the geochron and above the Northern Hemisphere Reference Line (Hart, 1984). In the $(^{206}Pb/^{204}Pb)_i$ vs. $(^{207}Pb/^{204}Pb)_i$ diagram (Fig. 7F), the studied samples form a close cluster within the field of arc magmas (Zartman and Doe, 1981). In the Fig. 7E, the Turnagöl samples fall within the fields of rocks from the lower crust (LC) described by Kempton et al. (1997) and are similar field of Torul samples (Kaygusuz et al., 2010).

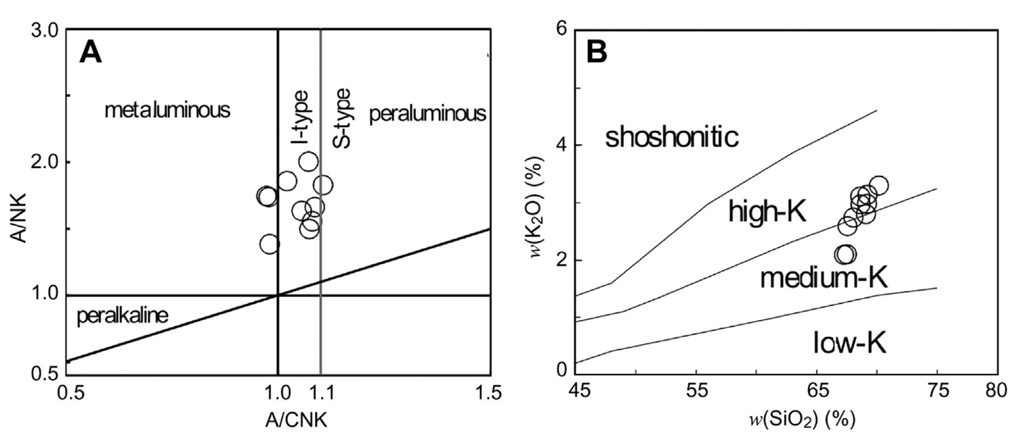

Figure 3. (A) A/CNK vs. A/NK, with field boundaries between I-type and S-type, according to Chappell and White (1974) and peraluminous and metaluminous fields of Shand (1947) and (B) $w(K_2O)$ vs. $w(SiO_2)$ diagram with field boundaries between medium-K, high-K and shoshonitic series according to Peccerillo and Taylor (1976). A/CNK = molar $Al_2O_3/(Na_2O + K_2O + CaO)$, A/NK = molar $Al_2O_3/(Na_2O + K_2O)$. Refer Fig. 2 for explanation.

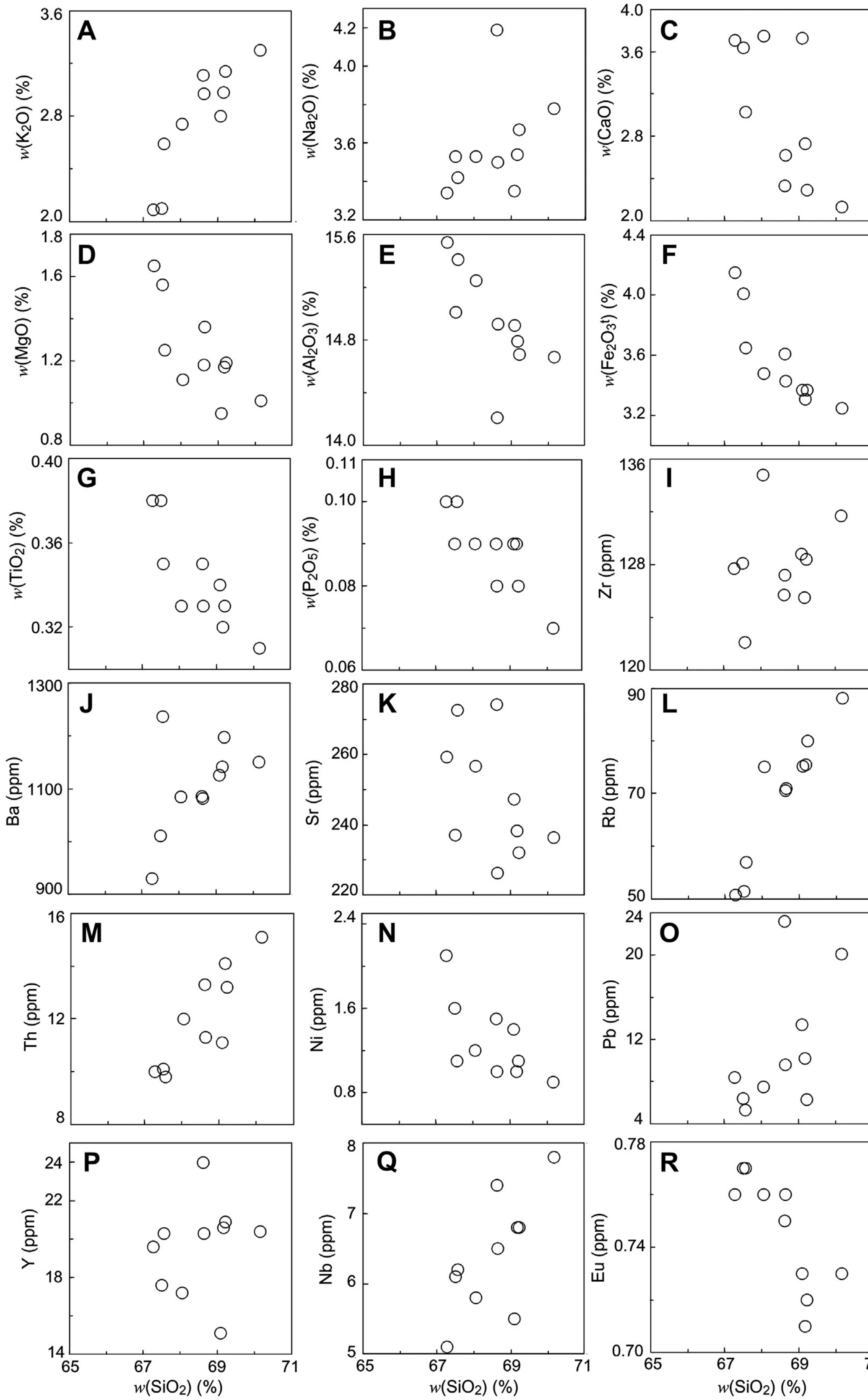

Figure 4. Variation diagrams of SiO_2 vs. major oxides (wt%) and trace elements (ppm) for samples from the Turnagöl intrusions. Refer Fig. 2 for explanation.

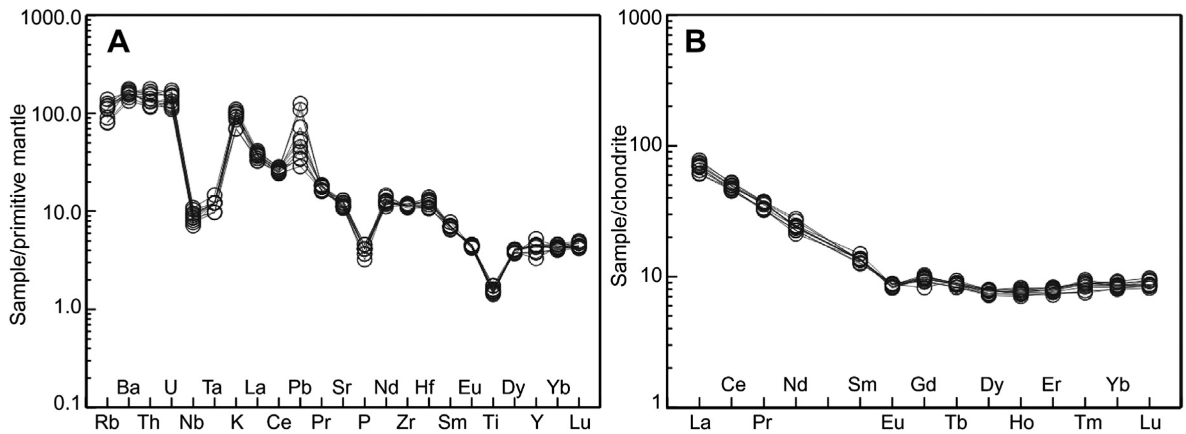

Figure 5. (A) Primitive mantle-normalized trace-element patterns (normalizing values from Sun and McDonough, 1989) and (B) Chondrite-normalized rare earth-element patterns (normalizing values from Taylor and McLennan, 1985) for samples from the Turnagöl intrusions. Refer Fig. 2 for explanation.

10. Oxygen isotopes

The whole-rock oxygen isotopic data are listed in Table 5 and plotted in Fig. 8A–D. The $\delta^{18}O$ values of the Turnagöl intrusion vary between +8.1‰ and +9.1‰, similar to those commonly found in I-type granitoids (e.g., Clarke, 1992). In the ε_{Nd_i}-$\delta^{18}O$ diagram (Fig. 8B), these samples define a weak trend of slightly increasing $\delta^{18}O$ with decreasing ε_{Nd_i}. A slightly positive correlation between the $\delta^{18}O$ values and SiO_2 is observed for the samples (Fig. 8C).

For comparison, the eastern Pontide arc-related plutonic rocks are plotted in the same diagram (Fig. 8D). The Turnagöl samples are found to have higher $\delta^{18}O$ and lower $(^{87}Sr/^{86}Sr)_i$ values than the Torul samples (Kaygusuz et al., 2008).

11. Discussion

11.1. Age constraints

In previous works, the emplacement age of the Cretaceous to Paleocene granitoids in the eastern Pontides was estimated from contact relationships, stratigraphic criteria, or biostratigraphic data. However, such data, are often imprecise or difficult to obtain due to rock deformation or tectonic displacement. Thus, an age reassessment in light of new geochronological data appears essential. Yılmaz (1977) determined a U-Th-Pb age of 142 Ma on granite samples from the Çaykara intrusion. Gedikoğlu (1979) gave K-Ar cooling ages ranging from 115 to 65 Ma on quartz diorite and granodiorite samples from the Harşit pluton. Giles (1974), Taner (1977), and Moore et al. (1980) obtained K-Ar cooling ages ranging from 132 to 62 Ma on granodiorite and tonalite samples from the İkizdere (Kaçkar) pluton. Moore et al. (1980) reported K-Ar cooling ages ranging from 84 to 71 Ma on a granodiorite sample from the Dereli intrusion. Jica (1986) determined a K-Ar cooling age of 68 Ma on granodiorite samples from the Kürtün pluton. Oyman et al. (1995) obtained K-Ar cooling ages ranging from 82 to 60 Ma from the Şebinkarahisar intrusions. Yılmaz-Şahin (2005) as well as Boztuğ and Harlavan (2008) gave K-Ar hornblende cooling ages ranging from 138 to 61 Ma on a granodiorite sample from the Boğalı and Uzuntarla intrusions of the Araklı-Trabzon region. Kaygusuz et al. (2009) determined a U-Pb zircon age of 82.7 ± 1.5 Ma on monzogranite samples from the Sarıosman pluton. Kaygusuz and Aydınçakır (2009) reported U-Pb zicon ages of 88.1 ± 1.7 and

Table 3
LA-ICP-MS U-Pb zircon dating results of the Turnagöl intrusions.

Spot	Measured ratios										Corrected ages (Ma)					
	$^{207}Pb/^{206}Pb$	1σ	$^{207}Pb/^{235}U$	1σ	$^{206}Pb/^{238}U$	1σ	$^{208}Pb/^{232}Th$	1σ	$^{238}U/^{232}Th$	1σ	$^{207}Pb/^{235}U$	1σ	$^{206}Pb/^{238}U$	1σ	$^{208}Pb/^{232}Th$	1σ
T86-01	0.04732	0.00133	0.07815	0.00223	0.01197	0.00016	0.00403	0.00006	1.6391	0.02	76	2	77	1	81	1
T86-02	0.07142	0.00125	0.12344	0.0023	0.01253	0.00016	0.00451	0.00005	0.99484	0.01	84	4	78	2	77.5	1
T86-03	0.04642	0.00210	0.08039	0.00362	0.01256	0.00019	0.00407	0.00009	1.79782	0.02	79	3	80	2	82	2
T86-04	0.05268	0.00208	0.08841	0.00348	0.01217	0.00018	0.00413	0.00009	1.86733	0.02	78	4	77	2	77	1
T86-05	0.04794	0.00126	0.08000	0.00214	0.01210	0.00016	0.00404	0.00006	1.50949	0.02	78	2	78	2	81	1
T86-06	0.04744	0.00151	0.07804	0.00250	0.01193	0.00017	0.00396	0.00006	1.25409	0.01	76	2	76	2	80	1
T86-07	0.04722	0.00117	0.07663	0.00195	0.01177	0.00016	0.00396	0.00005	1.38852	0.01	75	2	75	2	80	1
T86-08	0.04721	0.00177	0.08164	0.00306	0.01254	0.00018	0.00395	0.00007	1.63663	0.02	80	3	80	2	80	1
T86-09	0.04924	0.00093	0.08271	0.00165	0.01218	0.00016	0.00397	0.00004	0.83535	0.01	75	3	78	2	78.4	1
T86-10	0.04739	0.00160	0.08002	0.00272	0.01224	0.00017	0.00394	0.00007	1.72501	0.02	78	3	78	2	79	1
T86-11	0.04787	0.00171	0.08360	0.00300	0.01266	0.00018	0.00425	0.00008	1.79574	0.02	82	3	81	2	86	2
T86-12	0.04948	0.00160	0.08632	0.00281	0.01265	0.00018	0.00410	0.00007	1.61840	0.02	84	3	81	2	83	1
T86-13	0.04916	0.00124	0.08333	0.00215	0.01229	0.00016	0.00405	0.00005	1.52172	0.02	81	2	79	1	82	1
T86-14	0.05427	0.00168	0.09394	0.00293	0.01255	0.00018	0.00425	0.00007	1.67485	0.02	82	4	80	3	79.6	1
T86-15	0.15889	0.00283	0.31943	0.00594	0.01458	0.0002	0.01062	0.00012	1.47949	0.01	78	3	80	2	86	3
T86-16	0.04972	0.00115	0.08033	0.00192	0.01172	0.00016	0.00377	0.00004	0.98667	0.01	78	2	75	2	76.1	1
T86-17	0.05041	0.00188	0.08712	0.00324	0.01253	0.00018	0.00392	0.00008	1.85421	0.02	85	3	80	2	79	2
T86-19	0.04779	0.00154	0.08166	0.00265	0.01239	0.00017	0.00394	0.00007	1.61340	0.02	80	2	79	2	79	1
T86-20	0.05180	0.00127	0.08613	0.00216	0.01206	0.00016	0.00406	0.00005	1.47402	0.01	75	3	77	2	77	1
T86-22	0.04921	0.00113	0.08162	0.00193	0.01203	0.00016	0.00404	0.00005	1.25134	0.01	80	2	77	1	81	1

Errors are 1σ, $^{206}Pb/^{238}U$ age (1) values used in the text as the weighted mean.

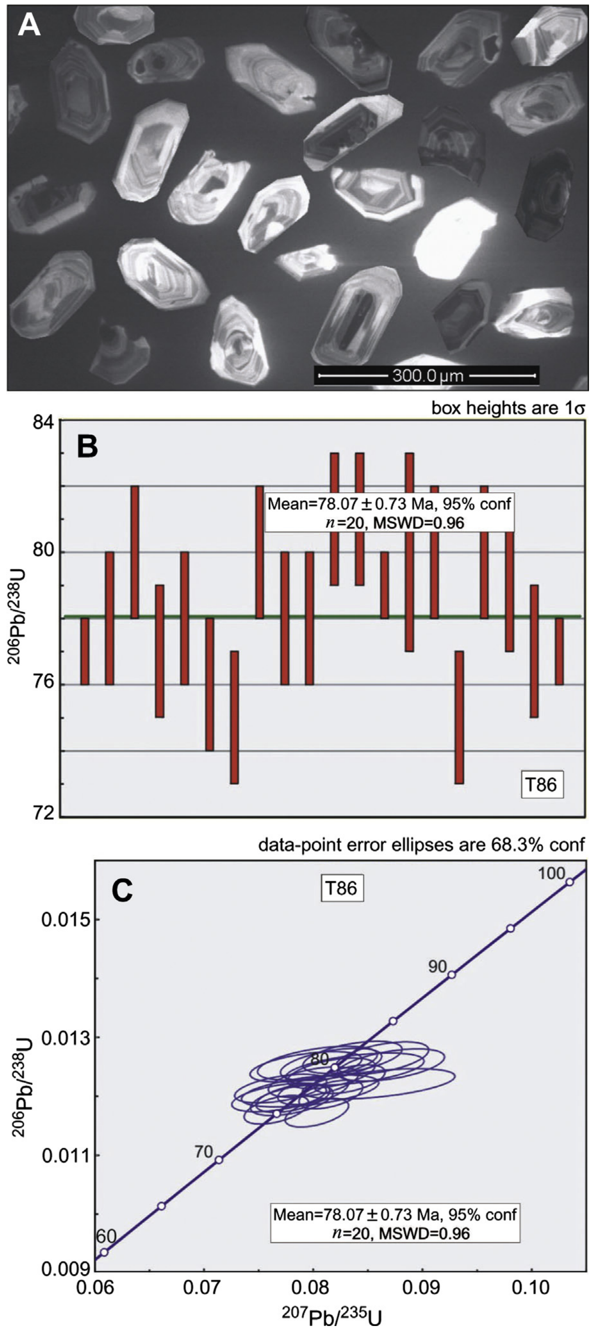

Figure 6. (A) CL images of zircons from sample T86; (B) and (C) Concordia diagram showing LA-ICP-MS U-Pb analyses of zircons from a granodiorite (sample T86) of the Turnagöl intrusions.

82.9 ± 1.3 Ma for tonalite and monzogranite samples, respectively, from the Dağbaşı pluton. Kaygusuz et al. (2008, 2010) determined U-Pb zircon ages ranging from 78.8 ± 1.2 Ma to 80.1 ± 1.6 Ma on monzogranite, quartz monzonite, and quartz monzodiorite samples, as well as an Rb/Sr age of 77.9 ± 0.3 Ma on syenogranite samples from the Torul pluton. Karslı et al. (2010) gave an Ar-Ar hornblende age of 79 Ma from the Harşit Pluton. Kaygusuz and Şen (2011) obtained a U-Pb zircon age of 79.3 ± 1.4 Ma on granodiorite samples from the Köprübaşı intrusion.

Prior to this study, information on the emplacement age of the Turnagöl intrusions was unsatisfactory for reconstructing their geological history. Based on contact relationships and stratigraphic criteria, an Upper Cretaceous and Eocene age was conjectured (Yalçınalp, 1992; Güven, 1993). However, our new LA-ICP-MS U-Pb zircon age on the Turnagöl intrusion is 78.07 ± 0.73 Ma (MSWD = 0.96). This age is more or less coeval with the emplacement age of the Torul, Sarıosman, Dağbaşı (Kaygusuz and Aydınçakır, 2009; Kaygusuz et al., 2010), and Harşit (Karslı et al., 2010) plutons.

11.2. Petrogenetic considerations

Petrogenetic models for the origin of felsic arc magmas fall into two broad categories: (1) felsic arc magmas are derived from basaltic parent magmas by FC or assimilation and FC (AFC) processes (e.g., Grove and Donnelly-Nolan, 1986; Bacon and Druitt, 1988); or (2) basaltic magmas provide heat for the partial melting of crustal rocks (e.g., Bullen and Clynne, 1990; Roberts and Clemens, 1993; Tepper et al., 1993; Guffanti et al., 1996). The first model has been considerably questioned because the granitoid and volcanic rocks of the study area as well as its adjacent regions are voluminous, and none has basaltic composition (all samples have an $w(SiO_2)$ content > 67%; Fig. 4). Such voluminous felsic magmas cannot be generated by differentiation of mantle-derived mafic magmas. The rock compositions do not represent a fractionation sequence from basalt to granodiorite or leucogranite. The low MgO concentrations (w(MgO) = 1.0%–1.7%; $Mg^{\#}$ = 22–29; Table 1) in the samples of the Turnagöl intrusion, as well as other geochemical parameters, rule out a direct derivation from the mantle wedge. A derivation of intrusions from mafic magmas through AFC processes can also be excluded because all rocks show little variation in their initial Sr-Nd isotope ratios with SiO_2 (Fig. 7B and C). Greater isotopic variability is expected if such a process had occurred. Granitoids representing mixtures of basaltic and granitic magmas are also unlikely because coeval basaltic members are lacking in the study area. There is abundant experimental evidence that the hydrous melting of basalt can produce tonalitic and trondhjemitic magmas (e.g., Wyllie, 1984) that may evolve (by FC and/or crustal contamination) toward more granitic compositions. The samples in the Fig. 4 plot present almost linear trends, and their bulk-rock composition can be related to partial melting (Caskie, 1984). Therefore, a crustal origin of magmas can be considered for the Turnagöl intrusion.

Table 4
Rb-Sr and Sm-Nd isotope data from the Turnagöl intrusions.

Sample	Type	Age (Ma)	Rb (ppm)	Sr (ppm)	$^{87}Rb/^{86}Sr$	$^{87}Sr/^{86}Sr$	2σ	$(^{87}Sr/^{86}Sr)_i$	Sm (ppm)	Nd (ppm)	$^{147}Sm/^{144}Nd$	$^{143}Nd/^{144}Nd$	2σ	$(^{143}Nd/^{144}Nd)_i$	ε_{Nd_i} [a]	T_{DM} [b]
T86	gd	78	41.50	237.10	0.5064	0.706818	0.000010	0.70626	2.89	16.10	0.1090	0.512458	0.000007	0.51240	−2.64	1.11
T88	gd	78	75.10	256.70	0.8464	0.707018	0.000010	0.70608	2.95	16.00	0.1120	0.512454	0.000009	0.51240	−2.75	1.11
T76	gd	78	71.00	226.30	0.9077	0.707182	0.000011	0.70618	3.11	18.90	0.0999	0.512428	0.000007	0.51238	−3.13	1.16
T73	gd	78	75.50	238.30	0.9166	0.707024	0.000010	0.70601	3.09	19.70	0.0952	0.512439	0.000010	0.51239	−2.87	1.14

[a] ε_{Nd_i} values are calculated based on present-day $^{147}Sm/^{144}Nd$ = 0.1967 and $^{143}Nd/^{144}Nd$ = 0.512638 (Jacobsen and Wasserburg, 1980).
[b] Single stage model age (T_{DM}), calculated with depleted mantle present-day parameters $^{143}Nd/^{144}Nd$ = 0.513151 and $^{147}Sm/^{144}Nd$ = 0.219, gd: granodiorite.

Table 5
Pb and $\delta^{18}O$ isotope data from the Turnagöl intrusions.

Sample	Type	Age (Ma)	$w(SiO_2)$ (%)	Pb (ppm)	U (ppm)	Th (ppm)	$^{206}Pb/^{204}Pb$	$(^{206}Pb/^{204}Pb)_i$	$^{207}Pb/^{204}Pb$	$(^{207}Pb/^{204}Pb)_i$	$^{208}Pb/^{204}Pb$	$(^{208}Pb/^{204}Pb)_i$	$\delta^{18}O$ (‰)
T86	gd	78	67.50	6.40	2.40	10.10	18.92	18.63	15.63	15.62	38.94	38.53	8.1
T88	gd	78	68.05	7.50	2.60	12.00	18.92	18.65	15.64	15.63	38.96	38.55	8.6
T76	gd	78	68.64	9.60	2.50	11.30	na	na	na	na	na	na	8.4
T73	gd	78	69.17	10.20	3.10	14.10	na	na	na	na	na	na	8.7
T78	gd	78	70.16	20.10	3.40	15.10	na	na	na	na	na	na	9.1

gd: granodiorite, na: not analyzed.

The partial melting of the lower crustal metabasalt yield a variety of granitoids whose compositions are controlled by the amount of H_2O (Tepper et al., 1993). Experimental studies have shown that amphibolites start to melt at relatively high temperatures (800–900 °C) and at pressures <1 GPa under anhydrous conditions, whereas dehydration melting commences at temperatures as low as 750 °C and at ~1 GPa (Wyllie and Wolf, 1993; Wolf and Wyllie, 1994; Lopéz and Castro, 2001). The

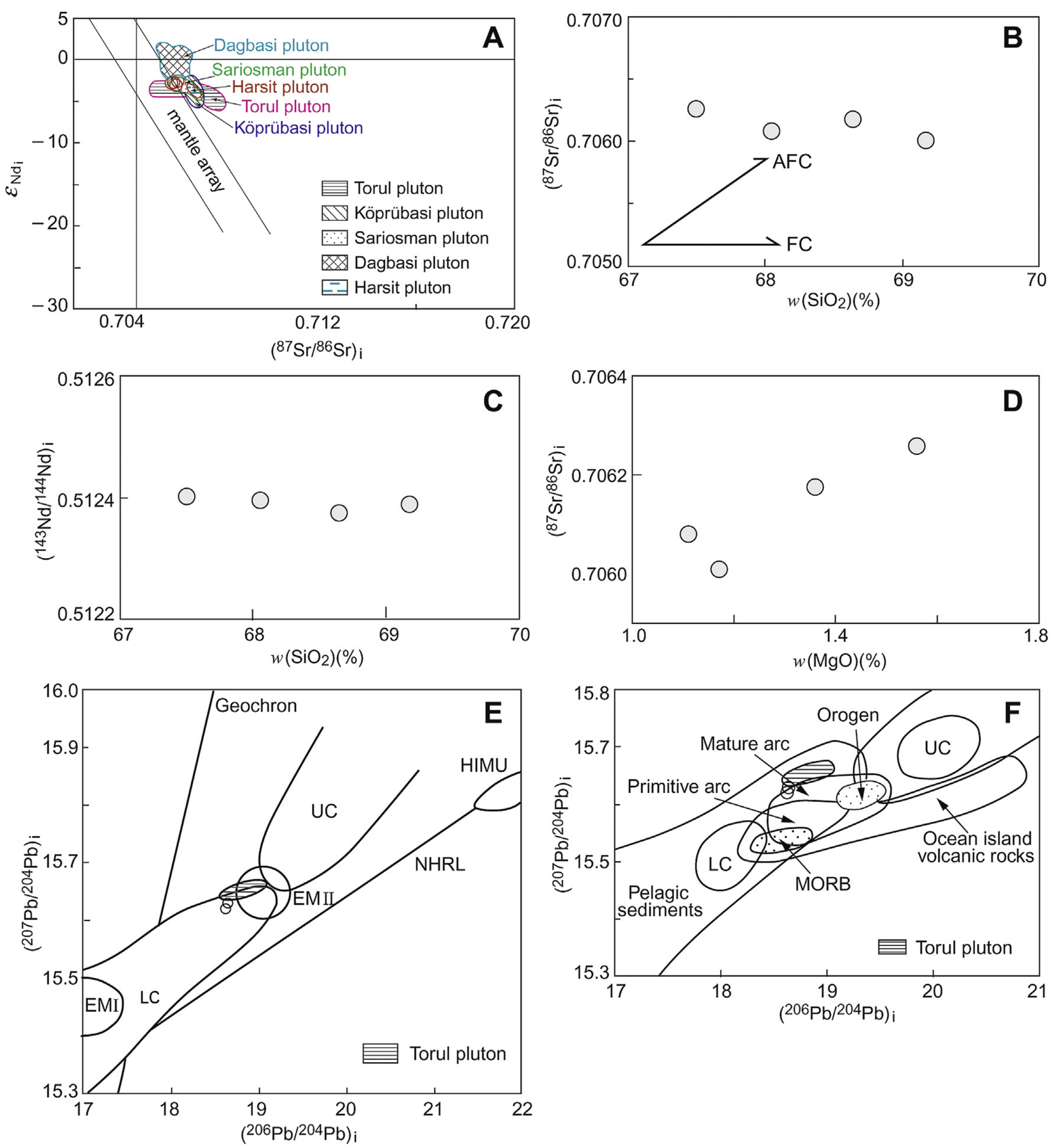

Figure 7. (A) ε_{Nd_i} values vs. $(^{87}Sr/^{86}Sr)_i$ ratio; (B) and (C) $(^{87}Sr/^{86}Sr)_i$ and $(^{143}Nd/^{144}Nd)_i$ vs. $w(SiO_2)$, respectively; (D) $(^{87}Sr/^{86}Sr)_i$ vs. $w(MgO)$; (E) and (F) Plot of $(^{207}Pb/^{204}Pb)_i$ vs. $(^{206}Pb/^{204}Pb)_i$ ratios. EM I – enriched mantle type I (Zindler and Hart, 1986); HIMU – High-μ ($\mu = {}^{238}U/^{204}Pb$) (Lustrino and Dallai, 2003); EM II – enriched mantle type II (enriched in Sr); LC – lower crust; NHRL – Northern Hemisphere Reference Line (Hart, 1984); UC – upper crust. The area of mantle (MORB), orogene, upper crust (UC), lower crust (LC), and pelagic sediments are from Zartman and Doe (1981). For explanation, refer Fig. 2.

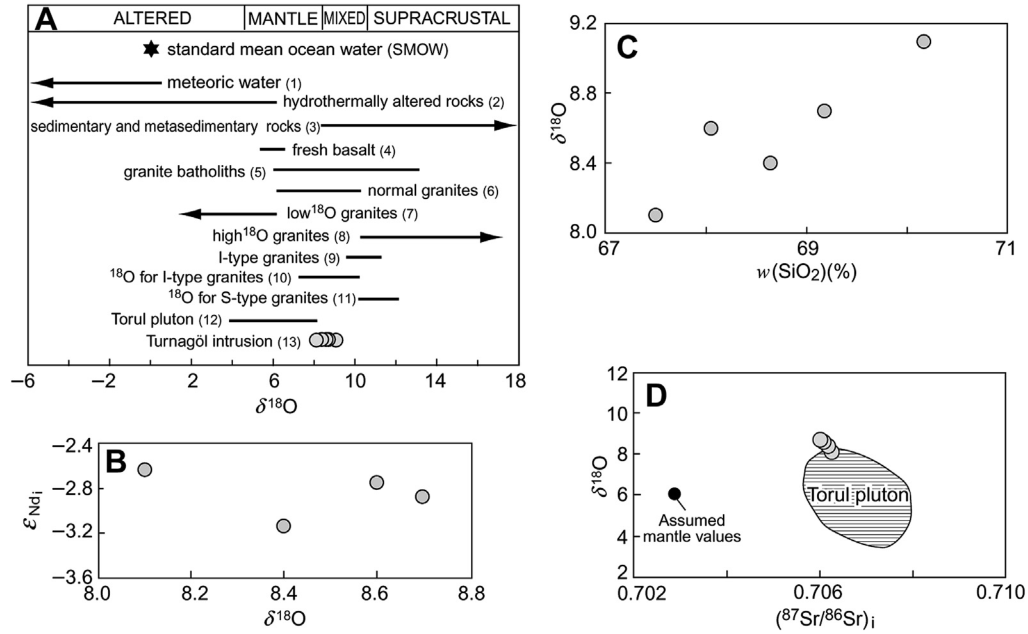

Figure 8. (A) Oxygen isotopic composition of the Turnagöl intrusions compared to those of typical terrestrial materials, granitoids and some S-I-A type granites; (B), (C) and (D) $\delta^{18}O$ values vs. ε_{Nd_i}, $w(SiO_2)$ and $(^{87}Sr/^{86}Sr)_i$, respectively. Data sources: 1 – Craig (1961); 2 – Ohmoto (1986); 3–5 – Taylor and Sheppard (1986); 6–8 – Taylor (1978); 9–11 – Harris et al. (1997); 12 – Kaygusuz et al. (2008). Dividing lines between altered, mixed, mantle and supracrustal rocks are taken from Whalen et al. (1996). Refer Fig. 2 for explanation.

specific melt composition resulting from the partial melting of the mafic lower crust is controlled by the water content, source composition, degree, and the *P-T* conditions of the melting (Rapp et al., 1991; Şen and Dunn, 1994; Wolf and Wyllie, 1994; Rapp and Watson, 1995; Winther, 1996; Lopéz and Castro, 2001). Based on data from the experimental partial melting of common crustal rocks, Roberts and Clemens (1993) stated that high-K, I-type, calc-alkaline granitoid magmas can be derived from the partial melting of hydrous, calc-alkaline mafic to intermediate metamorphic rocks in the crust. Recent experimental data have also shown that the partial melting of the mafic lower crust can generate melts of metaluminous granitic composition, and that the melt composition is largely independent of the degree of partial melting (Rushmer, 1991; Roberts and Clemens, 1993; Tepper et al., 1993; Wolf and Wyllie, 1994; Rapp and Watson, 1995).

11.3. FC and crustal contamination

Major and trace element variation trends (Fig. 4) bear evidence that FC has occurred during the evolution of the Turnagöl intrusion. The decrease in CaO, MgO, Al_2O_3, Fe_2O_3, TiO_2, P_2O_5, and Sr, as well as the increase of K_2O and Rb with increasing silica (Fig. 4), is related to the fractionation of plagioclase, hornblende, apatite, and titanite. Plagioclase fractionation results in lower abundances of Ba and Sr, low Sr/Nd ratios, as well as negative Eu anomalies in the chondrite-normalized REE patterns of the melts. The fractionation of hornblende causes an increase in the LREE/HREE in the residual melt, but a concave-upward shape (e.g., Romick et al., 1992) characterizes the resulting chondrite-normalized REE pattern of the melt. The increase in K_2O and Rb with increasing silica indicates that K-feldspar and biotite were not early-fractionation phases. This finding is in line with the late appearance of both minerals in the crystallization sequence. The depletion of P results from the removal of apatite during FC. The negative Ti anomalies in the spidergrams (Fig. 5) are consistent with titanite or titanomagnetite fractionation. The fractionation of accessory phases such as zircon, allanite, and titanite can account for the depletion of Zr and Y.

In addition to FC, crustal contamination can also be an important process during the evolution of magmatism in active continental margins. The continental crust has highly fractionated and enriched LREE, flat HREE, as well as a positive Pb anomaly, but negative Nb-Ta anomalies (Taylor and McLennan, 1985). The Turnagöl intrusion rocks are characterized by pronounced negative Nb-Ta and positive Pb anomalies (Fig. 5A), thus implying the subduction signature and a possible minor amount of crustal contribution in their evolution. In Fig. 7B–D, the $(^{87}Sr/^{86}Sr)_i$ and $(^{143}Nd/^{144}Nd)_i$ ratios are plotted against SiO_2 and MgO to evaluate the role of FC or AFC processes. The positive and negative trends indicate that the magmas were affected by AFC processes, whereas the nearly constant trends indicate significant FC. The $(^{143}Nd/^{144}Nd)_i$ and $(^{87}Sr/^{86}Sr)_i$ contents of the Turnagöl samples vs. SiO_2 exhibit nearly constant trends (Fig. 7B and C). The $(^{87}Sr/^{86}Sr)_i$ ratios are somewhat positively correlated with MgO (Fig. 7D).

11.4. Source rocks of the Turnagöl intrusion

The Turnagöl intrusion, composed of medium- to high-K calc-alkaline rocks, is characterized by pronounced negative Sr, Nb, Ta, and Ti anomalies but enriched Rb, Th, K, and Pb anomalies. These features are compatible to those of typical crustal melts, e.g., granitoids of the Lachlan Fold belt (Chappell and White, 1992) and Himalayan leucogranites (Harris et al., 1986; Searle and Fryer, 1986). Therefore, a derivation from crustal sources is apparent.

Several experimental studies (Wolf and Wyllie, 1994; Rapp and Watson, 1995) have shown that extremely high temperatures in excess of ~1100 °C are needed to produce mafic metaluminous low-silica (~58 wt.%) melts by the dehydration melting of metabasic crustal rocks. The compositional differences among magmas produced by the partial melting of different source rocks, such as amphibolites, metagraywackes, tonalitic gneisses, and metapelites, under variable melting conditions, may be visualized in terms of molar oxide ratios or major oxide ratios (Fig. 9). The dehydration melting of metapelites and metagraywackes (Rapp et al., 1991; Rapp, 1995; Rapp and Watson, 1995) yields higher values of $Mg^{\#}$,

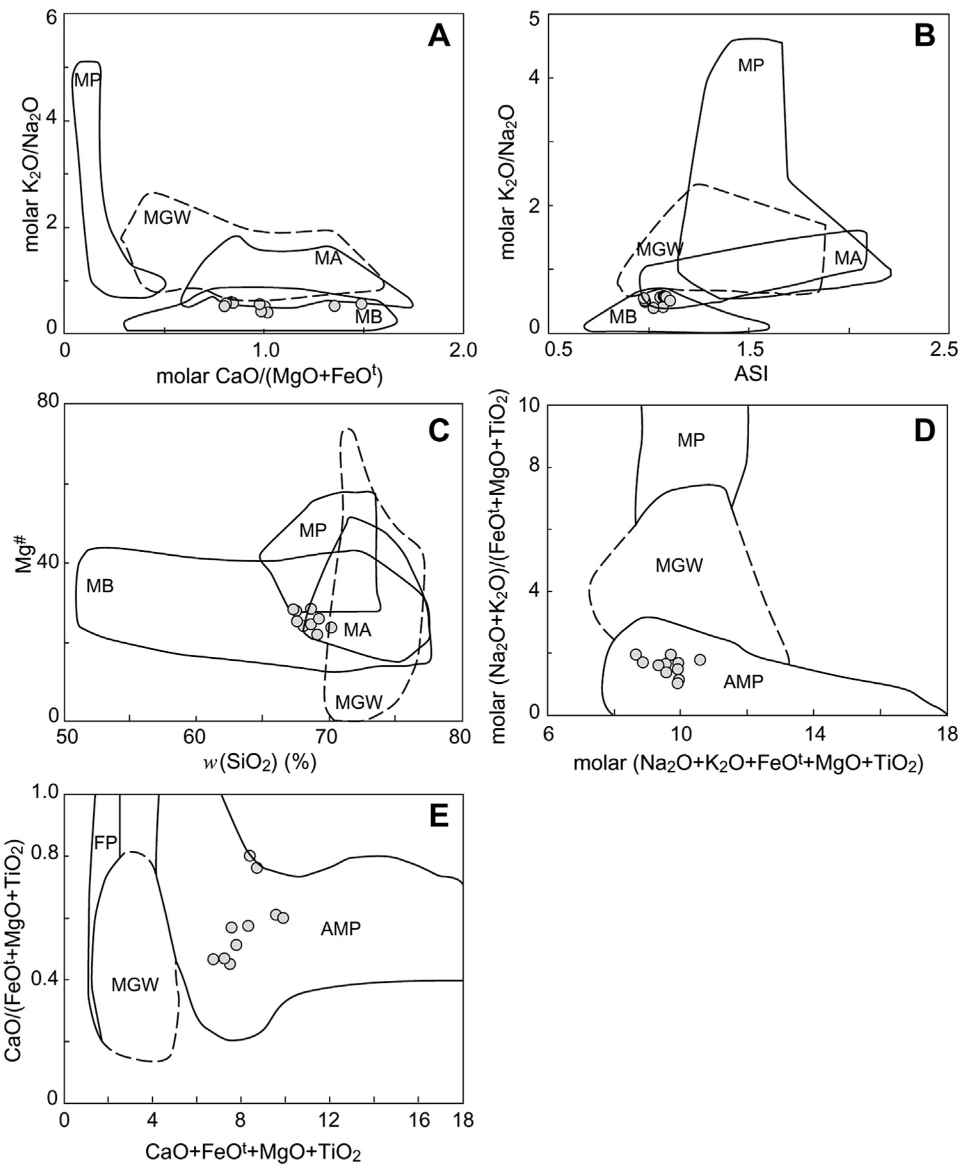

Figure 9. Chemical composition of the Turnagöl intrusions: outlined fields denote compositions of partial melts obtained in experimental studies by dehydration melting of various bulk compositions. MB, metabasalts (solid line); MA, metaandesites (solid line); MGW, metagreywackes (dashed line); MP, metapelites (solid line); FP, felsic pelites (solid line); AMP, amphibolites (solid line). Data sources: Vielzeuf and Holloway (1988); Patiño Douce and Johnston (1991); Rapp et al. (1991); Gardien et al. (1995); Rapp (1995); Rapp and Watson (1995); Patiño Douce and Beard (1996); Stevens et al. (1997); Skjerlie and Johnston (1996); Patiño Douce (1997); Patiño Douce and McCarthy (1998); Patiño Douce (1999). Consult Fig. 2 for explanation.

K_2O/Na_2O and $(Na_2O + K_2O)/(FeO^t + MgO + TiO_2)$, but lower values of $(CaO + FeO^t + MgO + TiO_2)$ compared with the investigated rocks (Fig. 9). The chemical compositions of the Turnagöl intrusions are thus rather compatible with an origin by dehydration melting from mafic lower crustal rocks. The chondrite-normalized REE diagrams (Fig. 5B) suggest that garnet is not stable in the source, whereas the negative Eu and Sr anomalies reveal that plagioclase is stable in the source of the Turnagöl intrusive rocks. A similar mechanism (partial melting from mafic lower crust) was also suggested for the origin of the arc-related Torul pluton by Kaygusuz et al. (2008) and Şebinkarahisar plutons by İlbeyli (2008) in the eastern Pontides.

12. Tectonic implications

Numerous studies suggest that trace elements can be used as discriminatory tools to distinguish among different tectonic settings of granitoid magmas. In the A/CNK vs. A/NK diagram (Fig. 3A), the samples plot within the I-type granite fields. In the FeO^t/MgO vs. $(Zr + Nb + Ce + Y)$ tectonic-discrimination diagram of Whalen et al. (1987), all samples are grouped within the I-type granite field (Fig. 10A). Applying the discrimination criteria of Pearce et al. (1984), all samples plot within the fields of volcanic-arc granites (VAG) (Fig. 10B). Difficulties exist in discriminating between collisional and arc-type granitoids (Brown et al., 1984; Pearce et al., 1984), and the Rb-Hf-Ta ratios of granitoids are often used to separate the collision-zone magmatism from the arc setting (Harris et al., 1986). The Rb/30-Hf-Ta×3 ternary diagram of Harris et al. (1986) provides a better distinction between volcanic-arc granites and pre-syn-late collisional granites. The Turnagöl samples plot within the VAG field of this diagram (Fig. 10C). Brown et al. (1984) established that the abundances of incompatible elements in granites can be correlated with the degree of arc maturity. An increase in the Nb and Y content with increasing Rb/Zr

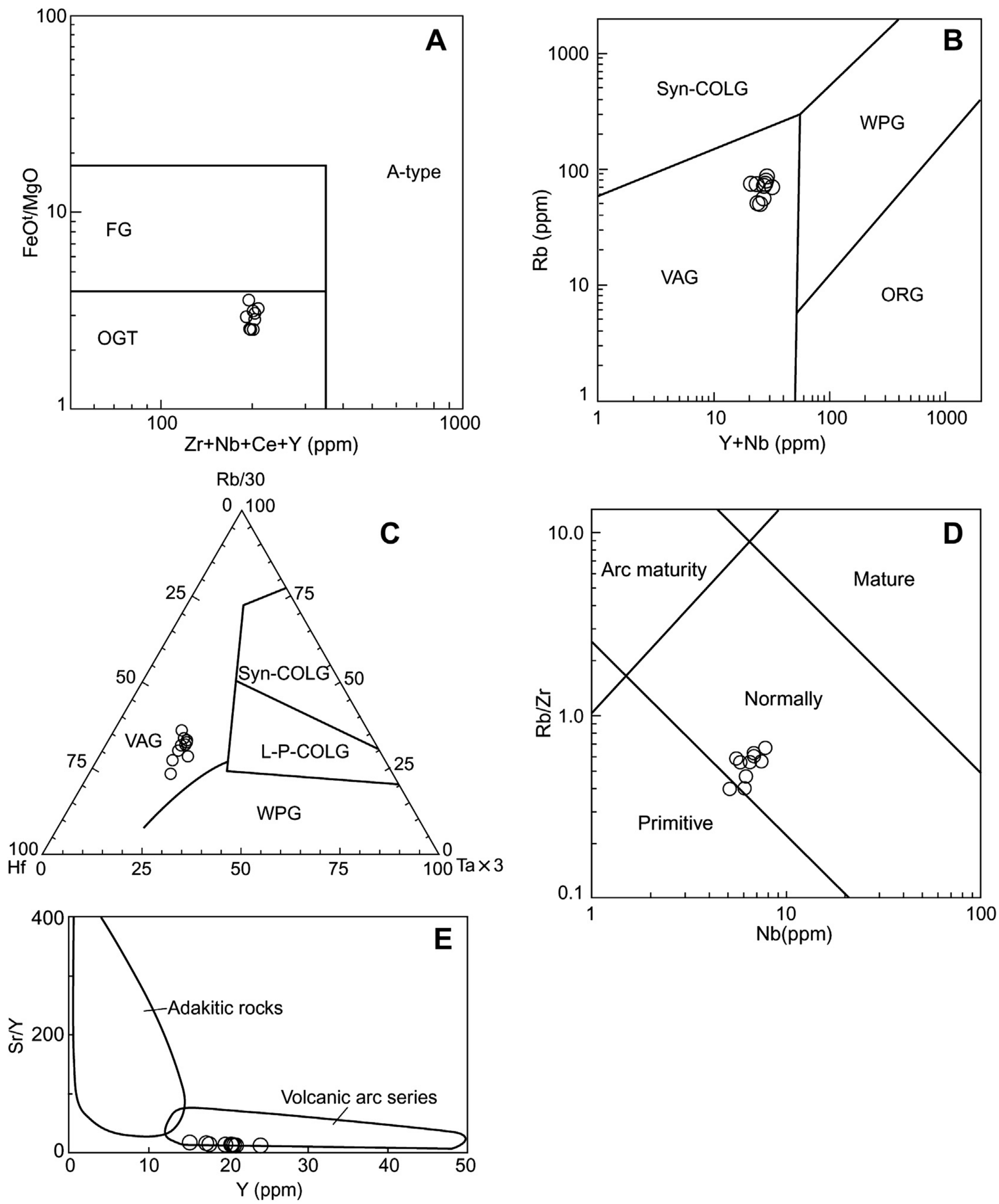

Figure 10. (A) FeO^t/MgO vs. (Zr + Nb + Ce + Y) classification diagram (Whalen et al., 1987); (B) Rb-(Y + Nb) discrimination diagrams (Pearce et al., 1984); (C) Rb/30-Hf-Ta×3 triangular diagram (Harris et al., 1986); (D) Nb vs. Rb/Zr diagram (Brown et al., 1984) and (E) Sr/Y vs. Y for samples from the Turnagöl intrusions. Adakites and island-arc fields are adopted from Drummond and Defant (1990). FG, fractionated granitoid; OGT, unfractionated; VAG, volcanic-arc granites; Syn-COLG, syn-collisional granites; WPG, within-plate granites; ORG, ocean-ridge granites; L-P-COLG, late-post-collisional granites. ASI (aluminium saturation index) = molar Al_2O_3/(Na_2O + K_2O + CaO). Refer Fig. 2 for explanation.

ratios is in accordance with the arc maturity, from primitive to mature. A comparison of the Turnagöl intrusion with the arc-type granitoids is presented in the Nb vs. Rb/Zr diagram (Fig. 10D). All samples from the pluton plot within the normal arc fields (Fig. 10E). On the Sr/Y vs. Y diagram (Fig. 10E), all samples plot within the low Sr/Y and high Y areas, which is similar to the modern island-arc field. The $(La/Yb)_n$ vs. Yb_n diagram (not shown) yields the same results.

13. Conclusions

The Turnagöl intrusion is considered a part of the late Cretaceous arc-related igneous activity in an active continental margin. It consists of granodiorite and yields an emplacement age of 78.07 ± 0.73 Ma by LA-ICP-MS U-Pb zircon dating.

The Turnagöl intrusion in the eastern Pontides is peraluminous to metaluminous, is medium- to high-K calc-alkaline, and has I-type characteristics. Its rocks are enriched in LILE and deficient in HFSE, showing features of arc-related intrusive rocks. Samples from the intrusion display concave-upward chondrite-normalized REE patterns with pronounced negative Eu anomalies. These features, combined with the decrease in CaO, MgO, Al_2O_3, Fe_2O_3, P_2O_5, TiO_2, and Sr with increasing silica, suggest that the intrusion underwent fractionation of plagioclase, hornblende, apatite, and titanite. All rock types of the pluton show a small range of Sr-Nd-Pb-O values.

The geochemical and isotopic data indicate that the intrusion was generated by the partial melting of mafic lower crustal sources. These plutons are related to the subduction of the Neo-Tethyan Ocean beneath the Eurasian plate during Cretaceous times, and were probably formed during the normal stage of a subduction setting.

Acknowledgments

We appreciate the help of Siebel Wolfgang and Elmar Reiter during isotope analyses. Thanks are due to Yener Eyuboğlu for editorial handling. Two anonymous reviewers are kindly thanked for their general improvement of the manuscript. Mürşit Öztürk and Metin Çiftçi are thanked for their help in the field. This research was supported by the grant No. 109Y052 from the Turkish Research Foundation (TÜBİTAK).

References

Akçay, M., Lermi, A., Van, A., 1998. Biogeochemical exploration in areas of dense vegetation: an orientation survey around the Kanköy Deposit (Trabzon, NE Turkey). Journal of Geochemical Exploration 63 (3), 173–187.

Altherr, R., Topuz, G., Siebel, W., Şen, C., Meyer, H.P., Satir, M., Lahaye, Y., 2008. Geochemical and Sr-Nd-Pb isotopic characteristics of Paleocene plagioleucitites from the eastern Pontides (NE Turkey). Lithos 105, 149–161.

Andersen, T., 2002. Correction of common lead in U-Pb analyses that do not report ^{204}Pb. Chemical Geology 192, 59–79.

Arslan, M., Aslan, Z., 2006. Mineralogy, petrography and whole-rock geochemistry of the Tertiary granitic intrusions in the eastern Pontides, Turkey. Journal of Asian Earth Sciences 27, 177–193.

Arslan, M., Tüysüz, N., Korkmaz, S., Kurt, H., 1997. Geochemistry and petrogenesis of the eastern Pontide volcanic rocks, Northeast Turkey. Chemie der Erde 57, 157–187.

Arslan, M., Şen, C., Aliyazıcıoğlu, İ., Kaygusuz, A., Aslan, Z., 2000. Trabzon ve Gümüşhane yörelerinde (KD, Türkiye) yüzeylenen Eosen (?) volkanitlerinin karşılaştırmalı jeolojisi, mineralojisi ve petrolojisi. Yerbilimleri ve Madencilik Kongresi Bildiriler Kitabı 1, 39–53.

Aydın, F., 2004. Mineral chemistry, petrology and petrogenesis of the Değirmendere Valley volcanics (Trabzon-Esiroğlu, NE-Turkey). Unpublished PhD Thesis, Karadeniz Technical University, Trabzon (in Turkish with English abstract).

Bacon, C.R., Druitt, T.H., 1988. Compositional evolution of the zoned calc-alkaline magma chamber of Mount Mazama, Crater Lake, Oregon. Contributions to Mineralogy and Petrology 98, 224–256.

Bektaş, O., Çapkınoğlu, Ş., 1997. Neptunian dikes and block tectonics in the eastern Pontide Magmatic Arc, NE Turkey: implications for the kinematics of the Mesozoic basins. Geosound 30, 451–461.

Bektaş, O., Van, A., Boynukalın, S., 1987. Jurassic volcanism and its geotectonics in the eastern Pontides (NE Turkey). Geological Bulletin of Turkey 30, 9–18.

Black, L.P., Kamo, S.L., Allen, C.M., Aleinikoff, J.N., Davis, D.W., Korsch, R.J., Foudoulis, C., 2003. TEMORA 1: a new zircon standard for Phanerozoic U–Pb geochronology. Chemical Geology 200, 155–170.

Boztuğ, D., Harlavan, Y., 2008. K-Ar ages of granitoids unravel the stages of Neo-Tethyan convergence in the eastern Pontides and central Anatolia, Turkey. International Journal of Earth Sciences 97, 585–599.

Boztuğ, D., Kuşçu, İ., Erçin, A.İ., Avcı, N., Şahin, S.Y., 2003. Mineral deposits associated with the pre-, syn- and post-collisional granitoids of the neo-Tethyan convergence system between the Eurasian and Anatolian plates in NE and Central Turkey. In: Eliopoulops, D. (Ed.), Mineral Exploration and Sustainable Development. Millpress, Rotterdam, pp. 1141–1144.

Boztuğ, D., Jonckheere, R., Wagner, G.A., Yeğingil, Z., 2004. Slow Senonian and fast Palaeocene–Early Eocene uplift of the granitoids in the Central eastern Pontides, Turkey: apatite fission-track results. Tectonophysics 382, 213–228.

Boztuğ, D., Erçin, A.İ., Kuruçelik, M.K., Göç, D., Kömür, İ., İskenderoğlu, A., 2006. Geochemical characteristics of the composite Kaçkar batholith generated in a Neo-Tethyan convergence system, eastern Pontides, Turkey. Journal of Asian Earth Sciences 27, 286–302.

Brown, G.C., Thorpe, R.S., Webb, P.C., 1984. The geochemical characteristics of granitoids in contrasting arcs and comments on magma sources. Journal of the Geological Society 141, 413–426.

Bullen, T.D., Clynne, M.A., 1990. Trace element and isotopic constraints on magmatic evolution at Lassen volcanic center. Journal of Geophysical Research 95, 19671–19691.

Caskie, D.R.M., 1984. Identification of petrogenetic processes using covariance plots of trace-element data. Chemical Geology 42, 325–341.

Chappell, B.W., White, A.J.R., 1974. Two contrasting granite types. Pacific Geology 8, 173–174.

Chappell, B.W., White, A.J.R., 1992. I- and S-type granites in the Lachlan Fold Belt. Transactions of the Royal Society of Edinburg, Earth Sciences 83, 1–26.

Clarke, D.B., 1992. Granitoid Rocks. Chapman and Hall, London, p. 283.

Clayton, R.N., Mayeda, T.K., 1963. The use of bromine pentafluoride in the extraction of oxygen from oxides and silicates for isotopic analysis. Geochimica et Cosmochimica Acta 27, 43–45.

Çoğulu, E. 1975. Gümüşhane ve Rize Granitik Plutonlarının Mukayeseli Petrojeolojik ve Jeokronolojik Etüdü [Petrogeologic and geochronologic investigation of Gümüşhane and Rize granitic plutons and their comparison]. Unpublished Dissertation Thesis, İstanbul Technical University (in Turkish with English abstract).

Craig, H., 1961. Standards for reporting concentrations of deuterium and oxygen 18 in natural waters. Science 133, 1833–1834.

Delaloye, M., Çoğulu, E., Chessex, R., 1972. Etude ge'ochronometrique des massifs cristallins de Rize et de Gümüşhane, Pontides Orientales (Turquie). In: CR des Sciences, 7, 2–3. SPHN, Geneve, pp. 43–52.

Dokuz, A., 2011. A slab detachment and delamination model for the generation of Carboniferous high-potassium I-type magmatism in the eastern Pontides, NE Turkey: the Köse composite pluton. Gondwana Research 19, 926–944.

Dokuz, A., Tanyolu, E., Genç, S., 2006. A mantle- and a lower crust-derived bimodal suite in the Yusufeli (Artvin) area, NE Turkey: trace element and REE evidence for subduction-related rift origin of Early Jurassic Demirkent intrusive complex. International Journal of Earth Sciences 95, 370–394.

Drummond, M.S., Defant, M.J., 1990. A model for trondhjemite-tonalite-dacite genesis and crustal growth via slab melting: Archean to modern comparisons. Journal of Geophysical Research 95, 21503–21521.

Eyuboğlu, Y., 2010. Late Cretaceous high-K volcanism in the eastern Pontide orogenic belt, and its implications for the geodynamic evolution of NE Turkey. International Geology Review 52 (2–3), 142–186.

Eyuboğlu, Y., Bektaş, O., Pul, D., 2007. Mid-Cretaceous olistostromal ophiolitic melange developed in the back-arc basin of the eastern Pontide magmatic arc, northeast Turkey. International Geology Review 49, 1103–1126.

Eyuboğlu, Y., Santosh, M., Chung, S.L., 2011a. Crystal fractionation of adakitic magmas in the crust-mantle transition zone: petrology, geochemistry and U-Pb zircon chronology of the Seme adakites, eastern Pontides, NE Turkey. Lithos 121, 151–166.

Eyuboğlu, Y., Santosh, M., Dudas, F.O., Chung, S.L., Akaryalı, E., 2011b. Migrating magmatism in a continental arc: geodynamics of the Eastern Mediterranean revisited. Journal of Geodynamics 52, 2–15.

Eyuboğlu, Y., Chung, S.L., Dudas, F.O., Santosh, M., Akaryali, E., 2011c. Transition from shoshonitic to adakitic magmatism in the eastern Pontides, NE Turkey: implications for slab window melting. Gondwana Research 19, 413–429.

Eyuboğlu, Y., Santosh, M., Chung, S.L., 2011d. Petrochemistry and U-Pb ages of adakitic intrusions from the Pulur massif (eastern Pontides, NE Turkey): implications for slab roll-back and ridge subduction associated with Cenozoic convergent tectonics in eastern Mediterranean. Journal of Geology 119, 394–417.

Eyuboğlu, Y., Santosh, M., Yi, K., Bektaş, O., Kwon, S., 2012. Discovery of Miocene adakitic dacite from the eastern Pontides Belt and revised geodynamic model for the late Cenozoic Evolution of eastern Mediterranean region. Lithos 146–147, 218–232.

Fayek, M., Kyser, T.K., 2000. Low temperature oxygen isotopic fractionation in the uraninite–UO_3–CO_2–H_2O system. Geochimica et Cosmochimica Acta 64 (13), 2185–2197.

Gardien, V., Thompson, A.B., Grujic, D., Ulmer, P., 1995. Experimental melting of biotite+plagioclase+quartz±muscovite assemblages and implications for crustal melting. Journal of Geophysical Research 100, 15581–15591.

Gedikoğlu, A., 1978. Harşit granit karmaşığı ve çevre kayaçları, Doçentlik Tezi, KTÜ Yer Bilimleri Fakültesi, Trabzon p. 161 (unpublished).

Gedikoğlu, A., 1979. Harşit (Giresun–Doğankent) granit karmaşığının jeokronolojik etüdü. Türkiye Jeoloji Bilimsel ve Teknik Kurultayı Bildiri Özleri Kitabı 33, 59–60.

Giles, D.L., 1974. Geology and mineralization of the Ulutaş copper–molybdenum prospect, mineral exploration in two areas. UNDP Technical Report 6, MTA, Ankara (unpublished).

Grove, T.L., Donnelly-Nolan, J.M., 1986. The evolution of young silicic lavas at Medicine Lake Volcano, California: implications for the origin of compositional gaps in calc-alkaline series lavas. Contribution to Mineralogy and Petrology 92, 281–302.

Guffanti, M., Clynne, M.A., Muffler, L.J.P., 1996. Thermal and mass implications of magmatic evolution in the Lassen volcanic region, California, and constraints on basalt influx to the lower crust. Journal of Geophysical Research 101, 3001–3013.

Güven, İ.H., 1993. 1:25000 Scale geology and compilation of the eastern Pontide. General Directorate of Mineral Research and Exploration (MTA) of Turkey, Ankara (unpublished).

Hanchar, J.M., Watson, E.B., 2003. Zircon saturation thermometry. In: Hanchar, J.M., Hoskin, P.W.O. (Eds.), Zircon. Rev in Mineralogy and Geochemistry, vol. 53. Mineralogical Society of America, Geochemical Society of America, pp. 89–112.

Harris, N.B.W., Pearce, J.A., Tindle, A.G., 1986. Geochemical Characteristics of Collision-zone Magmatism. In: Geological Society of London, Special Publication 19, pp. 67–81.

Harris, C., Faure, K., Diamond, R.E., Scheepers, R., 1997. Oxygen and hydrogen isotope geochemistry of S- and I-type granitoids: the Cape granite suite, South Africa. Chemical Geology 143, 95–114.

Harrison, T.M., Watson, E.B., 1984. The behaviour of apatite during crustal anatexis: equilibrium and kinetic considerations. Geochimica et Cosmochimica Acta 48, 1467–1477.

Hart, S.R., 1984. A large scale isotope anomaly in the Southern Hemisphere mantle. Science 309, 753–757.
İlbeyli, N., 2008. Geochemical characteristics of the Şebinkarahisar granitoids in the eastern Pontides, northeast Turkey: petrogenesis and tectonic implications. International Geology Review 50, 563–582.
Jacobsen, S.B., Wasserburg, G.J., 1980. Sm–Nd isotopic evolution of chondrites. Earth and Planetary Science Letters 50, 139–155.
Jica, 1986. The Republic of Turkey Report on the Cooperative Mineral Exploration of Gümüşhane Area, Consolidated Report. Japanese International Cooperation Agency, Metal Mining Agency of Japan.
Karslı, O., Aydın, F., Sadıklar, M.B., 2004. Magma interaction recorded in plagioclase zoning in granitoid systems, Zigana Granitoid, eastern Pontides, Turkey. Turkish Journal of Earth Sciences 13, 287–305.
Karslı, O., Chen, B., Aydin, F., Şen, C., 2007. Geochemical and Sr-Nd-Pb isotopic compositions of the Eocene Dölek and Sarıçiçek Plutons, Eastern Turkey: implications for magma interaction in the genesis of high-K calc-alkaline granitoids in a post-collision extensional setting. Lithos 98, 67–96.
Karslı, O., Dokuz, A., Uysal, İ., Aydın, F., Chen, B., Kandemir, R., Wijbrans, J., 2010. Relative contributions of crust and mantle to generation of Campanian high-K calc-alkaline I-type granitoids in a subduction setting, with special reference to the Harşit Pluton, Eastern Turkey. Contribution to Mineralogy and Petrology 160, 467–487.
Kaygusuz, A., Aydınçakır, E., 2009. Mineralogy, whole-rock and Sr–Nd isotope geochemistry of mafic microgranular enclaves in Cretaceous Dağbaşı granitoids, eastern Pontides, NE Turkey: evidence of magma mixing, mingling and chemical equilibration. Chemie der Erde 69, 247–277.
Kaygusuz, A., Şen, C., 2011. Calc-alkaline I-type plutons in the eastern Pontides, NE Turkey: U-Pb zircon ages, geochemical and Sr-Nd isotopic compositions. Chemie der Erde 71, 59–75.
Kaygusuz, A., Siebel, W., Şen, C., Satır, M., 2008. Petrochemistry and petrology of I-type granitoids in an arc setting: the composite Torul pluton, eastern Pontides, NE Turkey. International Journal of Earth Sciences 97, 739–764.
Kaygusuz, A., Chen, B., Aslan, Z., Wolfgang, S., Şen, C., 2009. U-Pb zircon SHRIMP ages, geochemical and Sr-Nd isotopic compositions of the Early Cretaceous I-type Sarıosman pluton, eastern Pontides, NE Turkey. Turkish Journal of Earth Sciences 18, 549–581.
Kaygusuz, A., Siebel, W., İlbeyli, N., Arslan, M., Satır, M., Şen, C., 2010. Insight into magma genesis at convergent plate margins – a case study from the eastern Pontides (NE Turkey). Neues Jahrbuch für Mineralogie Abhandlungen 187 (3), 265–287.
Kaygusuz, A., Arslan, M., Wolfgang, S., Şen, C., 2011. Geochemical and Sr-Nd isotopic characteristics of post-collisional calc-alkaline volcanics in the eastern Pontides (NE Turkey). Turkish Journal of Earth Sciences 20, 137–159.
Kaygusuz, A., Arslan, M., Wolfgang, S., Sipahi, F., İlbeyli, N., 2012. Geochronological evidence and tectonic significance of Carboniferous magmatism in the southwest Trabzon area, eastern Pontides, Turkey. International Geology Review 54 (15), 1776–1800.
Kempton, P.D., Downes, H., Embey-Istzin, A., 1997. Mafic granülite xenoliths in Neogene alkali basalts from the Western Pannonian Basin: insights into the lower crust of a collapsed orogen. Journal of Petrology 38, 941–970.
Ketin, İ., 1966. Anadolunun tektonik birlikleri [Tectonic units of Anatolia]. MTA Dergisi 66, 22–34.
Korkmaz, S., Tüysüz, N., Er, M., Musaoğlu, A., Keskin, İ., 1995. Stratigraphy of the eastern Pontides, NE Turkey. In: Erler, A., Ercan, T., Bingöl, E., Örçen, S. (Eds.), Proceedings of the International Symposium of the Geology of the Black Sea Region, pp. 59–68.
Lopéz, S., Castro, A., 2001. Determination of the fluid-absent solidus and supersolidus phase relationships of MORB-derived amphibolites in the range 4–14 kbar. American Mineralogist 86, 1396–1403.
Ludwig, K.R., 2003. Isoplot 3.0: A Geochronological Toolkit for Microsoft Excel. Berkeley Geochronology Center. Special Publication No. 4.
Lustrino, M., Dallai, L., 2003. On the origin of EM-I end-member. Neues Jahrbuch für Mineralogie Abhandlungen 179 (1), 85–100.
Middlemost, E.A.K., 1994. Naming materials in the magma/igneous rock system. Earth Science Review 37, 215–224.
Miller, C.F., Meschter McDowell, S., Mapes, R.W., 2003. Hot and cold granites? Implications of zircon saturation temperatures and preservation of inheritance. Geology 31, 529–532.
Moore, W.J., Mckee, E.H., Akıncı, Ö., 1980. Chemistry and Chronology of Plutonic Rocks in the Pontid mountains, Northern Turkey. Symposium of European Copper Deposits, Belgrade. 209–216.
Ohmoto, H., 1986. Systematics of metal ratios and sulfur isotopic ratios in low-temperature base metal deposits. Terra Cognita 6, 134–135.
Okay, A., Şahintürk, Ö., 1997. Geology of the eastern Pontides. In: Robinson, A.G. (Ed.), Regional and Petroleum Geology of the Black Sea and Surrounding Region. American Association Petroleum Geologist Memoir 68, pp. 291–311.
Oyman, T., Delaloye, M., Piskin, O., Calapkulu, F., 1995. Petrochemical and K-Ar radiometric investigations of granitoids from Sebinkarahisar area (Giresun-Turkey). In: Proceedings of International Earth Sciences Congress on Aegean Region. Dokuz Eylül University Publication 2, pp. 429–439.
Özsayar, T., Pelin, S., Gedikoğlu, A., 1981. Doğu Pontidler'de Kretase [Cretaceous in the eastern Pontides]. KTU Yer Bilimleri Dergisi 1, 2, p. 65–114.
O'Neil, J.R., Taylor Jr., H.P., 1969. Oxygen isotope fractionation between muscovite and water. Journal of Geophysical Research 74, 6012–6021.
Patiño Douce, A.E., 1997. Generation of metaluminous A-type granites by low-pressure melting of calc-alkaline granitoids. Geology 25, 743–746.
Patiño Douce, A.E., 1999. What do experiments tell us about the relative contributions of crust and mantle to the origin of granitic magmas? In: Castro, A., Fernandez, C., Vigneresse, J.L. (Eds.), Understanding Granites: Integrating New and Classical Techniques. Geological Society of London, Special Publication 168, pp. 55–75.
Patiño Douce, A.E., Beard, J.S., 1996. Effects of P, $f(O_2)$ and Mg/Fe ratio on dehydration melting of model metagreywackes. Journal of Petrology 37, 999–1024.
Patiño Douce, A.E., Johnston, A.D., 1991. Phase equilibria and melt productivity in the pelite system: implications for the origin of peraluminous granitoids and aluminous granulites. Contributions to Mineralogy and Petrology 107, 202–218.
Patiño Douce, A.E., McCarthy, T.C., 1998. Melting of crustal rocks during continental collision and subduction. In: Hacker, B.R., Liou, J.G. (Eds.), When Continents Collide: Geodynamics and Geochemistry of Ultra-high Pressure Rocks. Kluwer, Academic Publisher, Dordrecht, pp. 27–55.
Pearce, J.A., Harris, N.B.W., Tindle, A.G., 1984. Trace element discrimination diagram for the tectonic interpretation of granitic rocks. Journal of Petrology 25, 956–983.
Peccerillo, R., Taylor, S.R., 1976. Geochemistry of Eocene calc-alkaline volcanic rocks from the Kastamonu area, northern Turkey. Contributions to Mineralogy and Petrology 58, 63–81.
Pupin, J.P., 1980. Zircon and granite petrology. Contributions to Mineralogy and Petrology 73, 207–220.
Rapp, R.P., 1995. Amphibole-out phase boundary in partially melted metabasalt, its control over liquid fraction and composition, and source permeability. Journal of Geophysical Research 100, 15601–15610.
Rapp, R.P., Watson, E.B., 1995. Dehydration melting of metabasalt at 8–32 kbar: implications for continental growth and crust-mantle recycling. Journal of Petrology 36, 891–931.
Rapp, R.P., Watson, E.B., Miller, C.F., 1991. Partial melting of amphibolite eclogite and the origin of Archean trondhjemites and tonalites. Precambrian Research 51, 1–25.
Roberts, M.P., Clemens, J.D., 1993. Origin of high-potassium, calc-alkaline, I-type granitoids. Geology 21, 825–828.
Robinson, A.G., Banks, C.J., Rutherford, M.M., Hirst, J.P.P., 1995. Stratigraphic and structural development of the eastern Pontides, Turkey. Journal of the Geological Society of London 152, 861–872.
Romick, J.D., Kay, S.M., Kay, R.W., 1992. The influence of amphibole fractionation on the evolution of calc-alkaline andesite and dacite tephra from the Central Aleutians, Alaska. Contributions to Mineralogy and Petrology 112, 101–118.
Rushmer, T., 1991. Partial melting of two amphibolites: contrasting experimental results under fluid-absent conditions. Contributions to Mineralogy and Petrology 107, 41–59.
Searle, M.P., Fryer, B.J., 1986. Garnet-, tourmaline- and muscovite bearing leucogranites, gneisses and migmatites of the higher Himalayas from Zanskar, Kulu, Lahoul and Kashmir. In: Coward, M.P., Ries, A.C. (Eds.), Collision Tectonics. Geological Society, Special Publication 19, pp. 185–202.
Shand, S.J., 1947. Eruptive Rocks. Their Genesis, Composition, Classification and Their Relation to Ore-deposits, third ed. J Wiley Sons, New York, p. 488.
Skjerlie, K.P., Johnston, A.D., 1996. Vapour-absent melting from 10 to 20 kbar of crustal rocks that contain multiple hydrous phases: implications for anatexis in the deep to very deep continental crust and active continental margins. Journal of Petrology 37, 661–691.
Stevens, G., Clemens, J.D., Droop, G.T.R., 1997. Melt production during granulite facies anatexis: experimental data from 'primitive' metasedimentary protoliths. Contributions to Mineralogy and Petrology 128, 352–370.
Sun, S.S., McDonough, W.F., 1989. Chemical and isotope systematics of oceanic basalts; implication for mantle compositions and processes. In: Saunders, A.D., Nory, M.J. (Eds.), Magmatism in the Ocean Basins. Journal of the Geological Society of London, Special Publication, vol. 42, pp. 313–345.
Taner, M.F., 1977. Etuda géologique et pétrographique de la région de Güneyce-İkizdere, située au sud de Rize (Pontides orientales, Turquie). Unpublished PhD Thesis, Universite de Geneve, p. 180.
Taylor, H.P., 1978. Oxygen and hydrogen isotope studies of plutonic granitic rocks. Earth and Planetary Science Letters 38, 177–210.
Taylor, S.R., McLennan, S.M., 1985. The Continental Crust: Its Composition and Evolution. Blackwell Publication, Oxford, p. 312.
Taylor, H.P., Sheppard, S.M.F., 1986. Igneous rocks I. Processes of isotopic fractionation and isotope systematics. In: Valley, J.W., Taylor Jr., H.P., O'Neil, J.R. (Eds.), Stable Isotopes in High Temperature Geological Processes. Reviews in Mineralogy, vol. 16, pp. 227–272.
Temizel, İ., Arslan, M., 2009. Mineral chemistry and petrochemistry of post-collisional Tertiary mafic to felsic cogenetic volcanics in the Ulubey (Ordu) area, eastern Pontides, NE Turkey. Turkish Journal of Earth Sciences 18, 29–53.
Temizel, İ., Arslan, M., Ruffet, G., Peucat, J.J., 2012. Petrochemistry, geochronology and Sr–Nd isotopic systematics of the Tertiary collisional and post-collisional volcanic rocks from the Ulubey (Ordu) area, eastern Pontide, NE Turkey: implications for extension-related origin and mantle source characteristics. Lithos 128, 126–147.
Tepper, J.H., Nelson, B.K., Bergantz, G.W., Irving, A.J., 1993. Petrology of the Chilliwack batholith, North Cascades, Washington: generation of calc-alkaline granitoids by melting of mafic lower crust with variable fugacity. Contribution to Mineralogy and Petrology 113, 333–351.
Tokel, S., 1977. Doğu Karadeniz Bölgesi'nde Eosen yaşlı kalk alkalen andezitler ve jeotektonizma [Eocene calc-alkaline andesites and geotectonism in the Eastern Black Sea region]. Türkiye Jeoloji Kurumu Bülteni 20, 49–54.

Topuz, G., Altherr, R., Kalt, A., Satır, M., Werner, O., Schwarz, W.H., 2004. Aluminous granulites from the Pulur complex, NE Turkey: a case of partial melting, efficient melt extraction and crystallization. Lithos 72, 183–207.
Topuz, G., Alther, R., Schwarz, W.H., Siebel, W., Satır, M., Dokuz, A., 2005. Post-collisional plutonism with adakite-like signatures: the Eocene Saraycık granodiorite (eastern Pontides, Turkey). Contributions to Mineralogy and Petrology 150, 441–455.
Topuz, G., Altherr, R., Schwarz, W.H., Dokuz, A., Meyer, H.P., 2007. Variscan amphibolitefacies metamorphic rocks from the Kurtoğlu metamorphic complex (Gümüşhane area, eastern Pontides, Turkey). International Journal of Earth Sciences 96, 861–873.
Topuz, G., Altherr, R., Siebel, W., Schwarz, W.H., Zack, T., Hasözbek, A., Barth, M., Satır, M., Şen, C., 2010. Carboniferous high-potassium I-type granitoid magmatism in the eastern Pontides: the Gümüşhane pluton (NE Turkey). Lithos 116, 92–110.
Vennemann, T.W., O'Neil, J.R., 1996. Hydrogen isotope fractionation between hydrous minerals and molecular hydrogen. Geochimica et Cosmochimica Acta 60, 2437–2451.
Vielzeuf, D., Holloway, J.R., 1988. Experimental determinations of the fluid-absent melting reactions in the pelitic system. Contributions to Mineralogy and Petrology 98, 257–276.
Watson, E.B., Harrison, T.M., 1983. Zircon saturation revisited: temperature and composition effects in a variety of crustal magma types. Earth and Planetary Science Letters 64, 295–304.
Wenner, D.B., Taylor Jr., H.P., 1971. Temperatures of serpentinization of ultramafic rocks based on $^{16}O/^{18}O$ fractionation between coexisting serpentine and magnetite. Contributions to Mineralogy and Petrology 32, 165–185.
Whalen, J.B., Currie, K.L., Chappell, B.W., 1987. A-type granites: geochemical characteristics, discrimination and petrogenesis. Contributions to Mineralogy and Petrology 95, 407–419.
Whalen, J.B., Jenner, G.A., Longstaffe, F.J., Robert, F., Gariepy, C., 1996. Geochemical and isotopic (O, Nd, Pb and Sr) constraints on A-type granite petrogenesis based on the Topsails igneous suite, Newfoundland Appalachians. Journal of Petrology 376, 7–60.
Wiedenbeck, M., Alle, P., Corfu, F., Griffin, W.L., Meier, M., Oberli, F., Vonquadt, A., Roddick, J.C., Speigel, W., 1995. Three natural zircon standards for U–Th–Pb, Lu–Hf, trace-element and REE analyses. Geostandard Newsletter 19, 1–23.
Winther, K.T., 1996. An experimentally based model for the origin of tonalitic and trondhjemitic melts. Chemical Geology 127, 43–59.
Wolf, M., Wyllie, P., 1994. Dehydration melting of solid amphibolite at 10 kb. The effect of temperature and time. Contributions to Mineralogy and Petrology 115, 369–383.
Wyllie, P.J., 1984. Constraints imposed by experimental petrology on possible and impossible magma sources and products. Transactions of the Royal Society of London A310, 439–456.
Wyllie, P.J., Wolf, M.B., 1993. Amphibolite dehydration-melting: sorting out the solidus. In: Prichard, H.M., Alabaster, T., Harris, N.B.W., Neary, C.R. (Eds.), Magmatic Processes and Plate Tectonics. Geological Society, London, Special Publication 76, pp. 405–416.
Yalçınalp, B., 1992. Güzelyayla (Maçka-Trabzon) Porfiri Cu-Mo Cevheleşmesinin Jeolojik Yerleşimi ve Jeokimyası. Unpublished PhD Thesis, KTÜ, Trabzon.
Yeğingil, Z., Boztuğ, D., Er, M., Oddone, M., Bigazzi, G., 2002. Timing of neotectonic fracturing by fission-track dating of obsidian in-filling faults in the İkizdere-Rize area, NE Black Sea region Turkey. Terra Nova 14 (3), 169–174.
Yücel, C., Arslan, M., Temizel, İ., Abdioğlu, E., 2011. Whole-rock chemostratigraphy of diverse magma series in the Tertiary alkaline volcanics of Trabzon-Giresun area, NE Turkey. Goldschmidt Conference Abstracts, Mineralogical Magazine, 2237.
Yılmaz, Y., 1972. Petrology and structure of the Gümüşhane Granite and surrounding rocks, north-eastern Anatolia. Unpublished PhD Thesis, University of London.
Yılmaz, İ., 1977. Çaykara granitlerinin petrojenetik ve jeokronometrik etüdü. Tübitak Doğa Bilim Dergisi 8, 29–35.
Yılmaz, S., Boztuğ, D., 1996. Space and time relations of three plutonic phases in the eastern Pontides, Turkey. International Geology Review 38, 935–956.
Yılmaz, C., Korkmaz, S., 1999. Basin development in the eastern Pontides, Jurassic to Cretaceous, NE Turkey. Zentralblatt für Geologie und Palaöntologie, Teil I 10–12, 1485–1494.
Yılmaz, Y., Tüysüz, O., Yiğitbaş, E., Genç, Ş.C., Şengör, A.M.C., 1997. Geology and tectonic evolution of the Pontides, regional and petroleum geology of the black sea and surrounding region. American Association Petroleum Geologists Memoir 68, 183–226.
Yılmaz, A., Adamia, S., Chabukiani, A., Chkhotua, T., Erdoğan, K., Tuzcu, S., Karabıyıkoğlu, M., 2000. Structural correlation of the southern Transcaucasus (Georgia)-eastern Pontides (Turkey). In: Bozkurt, E., Winchester, J.A., Piper, J.D.A. (Eds.), Tectonics and Magmatism in Turkey and Surrounding Area. Geological Society, London, Special Pub. 173, pp. 171–182.
Yılmaz-Şahin, S., 2005. Transition from arc- to post-collision extensional setting revealed by K–Ar dating and petrology: an example from the granitoids of the eastern Pontide igneous Terrane, Araklı-Trabzon, NE Turkey. Geological Journal 40, 425–440.
Yılmaz-Şahin, S., Güngör, Y., Boztuğ, D., 2004. Comparative petrogenetic investigation of Composite Kaçkar Batholith granitoids in Eastern Pontide magmatic arc-Northern Turkey. Earth Planets Space 56, 429–446.
Zartman, R.E., Doe, B.R., 1981. Plumbotectonics. The model. Tectonophysics 75, 135–162.
Zindler, A., Hart, S.R., 1986. Chemical geodynamics. Annual Review Earth Planetary Science 14, 493–571.
Şen, C., 2007. Jurassic volcanism in the eastern Pontides: is it rift related or subduction related? Turkish Journal of Earth Sciences 16, 523–539.
Şen, C., Dunn, T., 1994. Dehydration melting of a basaltic composition amphibolite at 1.5 and 2.0 GPa: implications for the origin of adakites. Contributions to Mineralogy and Petrology 117, 394–409.
Şen, C., Arslan, M., Van, A., 1998. Geochemical and petrological characteristics of the Pontide Eocene (?) alkaline province, NE Turkey. Turkish Journal of Earth Sciences 7, 231–239.
Şengör, A.M.C., Özeren, S., Genç, T., Zor, E., 2003. East Anatolian high plateau as a mantle-supported, North–South shortened domal structure. Geophysical Research Letter 30 (24), 8045. http://dx.doi.org/10.1029/2003GL017858.